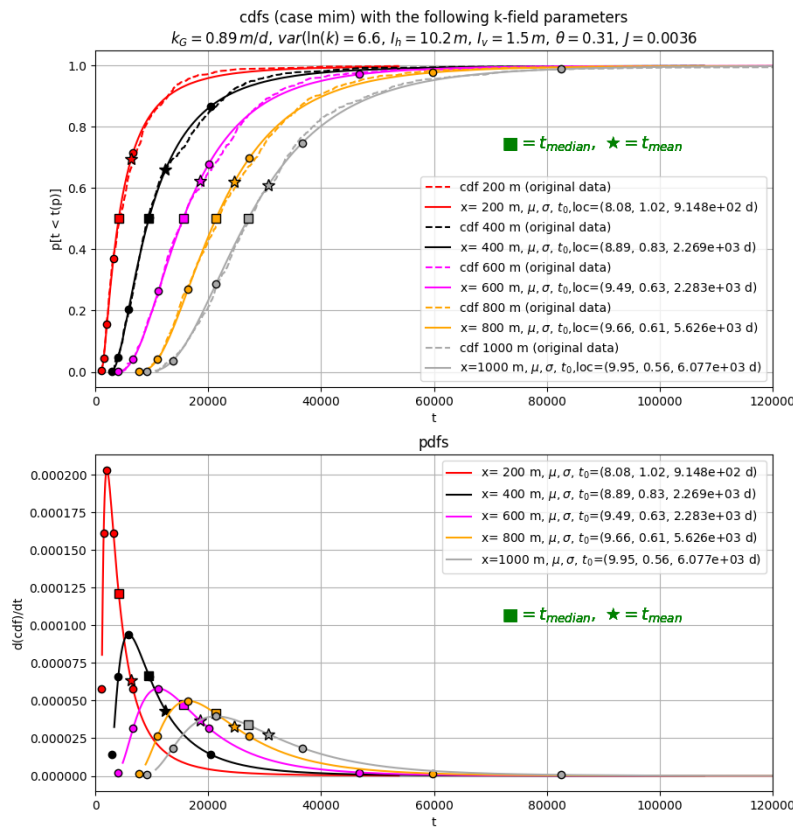


Dispersion: the effects of aquifer heterogeneity

prof. dr.ir. T.N.Olsthoorn

2025-04-23



Contents

1	Introduction	2
2	Analysis of advection-dominated dispersion using particle tracking in heterogeneous aquifers in 2D vertical cross sections	4
3	Literature discussion	5
4	Cross sections	7
4.1	Introduction	7
4.2	Generating cross sections	8

4.3	Cross section according to De Lange	9
4.4	More elaborate cross sections	9
4.5	Going fully geostatistical	9
4.6	Finally still lacking the third dimension	9
5	Cross section simulations	9
5.1	Basic properties	9
5.2	Made cross section as applied by Fiori et al (2012)	10
5.3	The same cross section with the same parameters except for a much lower variance of the conductivity, namely $\text{var}(\ln(k))$ is 1.1 instead of 6.6	15
5.4	Regular conductivity field as exponential random field with the same parameters as used in the MIM model of section 5.2.	20
5.5	A purely random field	25
5.6	Aquifer according to De Lange	30
5.7	Test case	35
6	Summarizing the discussion on dispersion	40
7	Summary and conclusions	42
8	Analysis of the lognormal distribution	43
References		45

1 Introduction

According to [De Lange (2020), De Lange (2022), De Lange (2025)] dispersion as we see it through sampling an aquifer, is almost completely caused by groundwater velocity variations on macro-scale and neither on velocity variations at the pore-scale nor on molecular particle movement caused by diffusion. Although pore-scale velocity differences always plays a role whenever groundwater is flowing, and diffusion even when it's not flowing, these two mechanisms are by many scholars believed to play such a small role in most real-world situations, that they can often be neglected when evaluating actual dispersion in the field or when modeling mass transport with dispersion.

So what is dispersion as we see it? Dispersion can be defined based on the gradual concentration increase, the reaching of a peak concentration followed by the slow decrease of a constituent when a well or an observation screen is frequently sampled. Dispersion can also be defined based on the average concentration over the height of the aquifer sampled by many vertically arranged small sampling screens or by sampling a fully penetrating well. With the latter method, using more than one well or series of sampling points at different spatial locations, we may try to outline the extent of a so-called plume of pollutant as it extends at a certain moment in time within the aquifer. We may try to accomplish the same thing by sampling one or multiple wells over time, taking into account the actual velocities of the groundwater, which are oftentimes difficult to determine.

Dispersion has mostly been defined as a process similar to diffusion, in that it is due to velocity differences at the pore-scale, which cause diffusion-aided mixing between adjacent streamlines and thus result in the observed spread of the pollutant both in the direction of the flow as well as perpendicular to it. In this traditional Fickian or Gaussian theory the spreading behaves as if it was driven purely by concentration gradients. In fact, without diffusion, at least, theoretically, a pollutant should not spread perpendicular to the streamlines in all cases where streamlines cannot cross each other. Streamlines can only cross each other in 3D space, and, therefore, such advection mechanisms cannot explain spreading of a pollutant perpendicular to streamlines in 2D space. Nevertheless streamlines can cross each other in 3D space (e.g. in aquifers with horizontal layers having main horizontal conductivity axes in different directions [Hemker and Bakker (2004)], [Jankovic et al. (2003), Jankovic et al. (2010)]). This eventually reduces the value of 2D dispersion analyses in a fundamental way as it remains impossible to determined the 3D impact happening in reality using a 2D simulation.

However, major velocity differences occur on macro scale, caused by differences of the hydraulic conductivity and or porosity on the scale of the sedimentation processes that originally formed the aquifer. Notice that we only consider aquifers consisting of sediments, that is, aquifers constructed of layers of particles of different sizes, as show up in borelogs and cross sections alike. These processes have built up the aquifer over large spans of geologic time, in layers, formed in different energetic environments, i.e. by water that carried different amounts of particles the size of which varied depending on the geologic and climatic circumstances. These circumstances have likely largely varied over the tens of thousands to millions of years, during which the aquifer was formed. Retracting seas during ice ages and rising land cause larger gradients of the earth's surface, due to which erosion increases and more and coarser sediments are laid out over extended areas, generally by wide braided rivers. Their sediments cause coarse-grained inclusions, which are detected in our current-day aquifers. During warmer, more vegetated eras, with higher ocean levels, rivers carry less and finer sediments, While meandering they cut into previously deposited sediment layers to form their characteristic patterns we now observe in cross sections. During cold windy periods with tundras as well as in dry deserts, large-scale areal transport and deposition of fine particles have formed often vast regions with moving dunes, which now show up in cross sections as often thick layers of overlapping sublayers of fine material. They are characterized by their upward curved patterns that witness the original horizontal progress of the dune-type deposits. Extended clay layers are generally caused by sea transgressions when climate warmed up or land sank. Or they were deposited by rivers that broke through their banks creating extended flood areas with little energy, which allowed fine particles to settle and to form river-clay deposits. We oftentimes witness all such previously active processes play out in the bore-hole profile or in natural or our own man-made cross sections. Looking at such profiles, we are watching how a vast number of geological processes has played out over hundreds of thousands to millions of years to form the aquifer at hand. No wonder the details of the flow of groundwater through an aquifer is complicated. When dealing with the groundwater head in an aquifer or at what rate we can extract water from it by a well, things are far less complicated due to natural averaging of the head between layers and the integration of the flow towards a well screen over all layers that intersect it. However, if we study the spread of pollutants within an aquifer, the details of the structure of the aquifer do matter. And it's obvious that the extremely wide variation of the conductivity within the aquifer, caused by the mentioned variety of sedimentation (and local erosion) processes, determine the spread of a pollutant more than velocity variations at the pore scale. As far as diffusion is concerned, it's important over the long run in stagnant situations and to allow constituents to jump between parallel stream lines. But on local scales and relative short, say sub-century time scales it tends to be of little importance.

While an aquifer tends to be built up over time by repeated fining-up sediment sequences, it is the braided river's coarse material deposition during cold periods that intersects such layered sequences and created inclusions with often sharply distinct hydraulic conductivities. To a somewhat lesser extent, we find „inclusions” (often called facies) caused by meandering rivers that cut into older layers while eroding their outer bends and at the same time depositing fresh material at their inner bends. This way, meandering rivers create their characteristic particle-band patterns in cross sections with their associated conductivity patterns. But we also encounter existing sediment packages that were disturbed, pushed up, shifted and partly or totally turned over by the heavy load of progressing land ice. When retracting and after melting, the deep valley space that was left over, was subsequently filled up by both erosion material from the pushed-up ridges and filled by fine material, especially caused by subsequent sea water rise. Of course, much more can be, and perhaps should be said about the characteristics of the cross sections we encounter in the field. Studying and describing them has been the focus of geologists and especially sedimentologists throughout the world over a long time. However using their descriptions to accurately model the heterogeneous conductivity field remains a challenge and is mostly not universally successful to say the least.

The fundamental consequence of attributing all „dispersion” to spatial conductivity variation in facies and inclusions, i.e. by neglecting pore- and grain-scale processes, is, that, in fact, no mixing can occur in the subsurface because it implies that every particle will stick to its own original streamline over its entire underground life. This would even be true when the streamline changes over time as a result of altered boundary conditions. Hence, with this assumption, all dispersion, i.e. mixing, occurs at the extraction point, where the extracted water is mixed in the screen or the well when pumping or just sampling it. Or, the water is mixed in the computer when we digitally mix the extracted water along the vertical at some point in the aquifer. There may be differences between physical and digital mixing, though. For instance,

the mixing in a well screen depends on the flow from each layer that intersects the assumed fully penetrating screen. This makes the layers with the highest conductivities dominant, as we often see when measuring the inflow to a well screen along its length. To get the right comparison, in the computer we must also take the afflux at each elevation along the well screen into consideration, which is not difficult to do. We can also do this over time. But in fact, when mixing the water vertically at a given point in the aquifer and a given point in time, we always mix water from layers with zero constituent concentration with water from layers with non-zero constituent concentration. And, under the assumption that only advection is active, a streamline either has exactly the same concentration it was given at the point of release after passing the point of none. This is a consequence of the assumption of zero mixing within the aquifer, which is what happens as particles stick to their streamline and pore-size processes are ignored. Hence, each streamline either carries a particle of the constituent or none at the moment and point of sampling.

When simulating discrete particle transport in the computer, the probability of hitting any particle at any streamline at the well exactly at the time of sampling may be vanishingly small. Therefore, we have to sample over a given amount of time, to capture at least some particles. Afterwards we integrate over time to get the cumulative probability distribution. Or rather considering an initially sharp front, we simply count the streamlines whose front particle has passed the observation point, sort these times and construct the cumulative breakthrough curve for this .

How then can we define dispersion when we consider it to be caused by advection through the heterogeneous aquifer alone? One way to do it, is by recording the particles that were initially released at one location and time, as they pass some point downstream. When the particles were initially distributed vertically in such a way that each of them represents the same fraction of water, while the total number of particles make up the entire groundwater flow, then we can construct the cumulative distribution of particles passing the observation location. The shape of this distribution represents the statistics of the advection-dispersion process in its entirety, and its derivative represents the density distribution, allowing for further statistical analysis and statistical generalization.

When we only take advection into account, it is fundamentally impossible to determine the dispersion after releasing particles at a single point and time, i.e. due to a concentration pulse. This impossibility is due to a sudden release of a given number of particles at a single point in the aquifer at a given point in time. This is so, because if this point source is theoretically a single point in the aquifer, then all particles would be on the same stream line and stick to it and would always travel at the same speed. Hence, no dispersion would ever occur within this framework. The fact alone that a point source does generate a growing plume in reality, implies that this concept of pure advection, may have its merits, but also has its limits.

Nobody can ignore that diffusion acts in groundwater, as it is caused by molecular movement, which is always present. The spread σ of an initial concentration pulse, or of an initially straight concentration front, is defined by the standard deviation $\sigma = \sqrt{2Dt}$ with D [L^2/T] the molecular diffusion coefficient. With a value of $D \approx 2 \times 10^{-9}$ [m^2/d], we have $\sigma \approx 0.25$ m in one year. This is not nothing. It spread will definitely does cause particles to step over to adjacent streamlines. In 100 years $\sigma \approx 2.5$ m and in 10000 years $\sigma \approx 25$ m. The latter is of the scale of the vertical extent of the aquifer itself. Hence, on the long run diffusion as a mechanism to spread out pollutants perpendicularly to the streamlines cannot be ignored and will limit the value of the pure advection approach to tens of years rather than hundreds or even thousands of years.

2 Analysis of advection-dominated dispersion using particle tracking in heterogeneous aquifers in 2D vertical cross sections

Assuming that dispersion is caused by macroscale velocity variations due to the aquifer's heterogeneous conductivity field, we can analyze it by means of particle tracking. In order to include diffusion (but still ignoring porescale velocity variations) we would have to include mass transport with diffusion, which is outside our current scope.

Even realizing its limits, we will stick with a vertical, i.e. 2D cross section of uniform height modeled with finite differences using a rectangular mesh with sub layers of equal height. The conductivity of each cell may be unique, and the vertical and horizontal conductivities may be different. Furthermore, also the porosity in each cell may be chosen to be unique. However, the variations of the porosity in a real aquifer tend to be small, even negligible compared to the variations in hydraulic conductivity. For this reason, without loss of

generality, we will use a constant porosity of around 35% throughout our analysis.

The boundary conditions of the modeled cross section are a fixed but different head at both ends. This would yield a uniform flow field when the aquifer were homogeneous. However, due to its heterogeneity, the flow field is far from homogeneous and will be determined by a steady-state computation with Modflow. The results allow us to visualize not only the lines of constant head, but also the lines of constant values of the stream function. The stream function allows us to determine uniquely the flow density and the flow direction at any point in the aquifer, even without particle tracking. The stream function permits us to determine the elevation of the release points of the particles such that each particle represents the same amount of discharge, which will guarantee keeping the mass balance also with particle tracking.

Particle tracking is done with Modpath7. Modpath guarantees that the governing differential equation of the discharge is fulfilled at every point within every cell of the model. This implies that, although the model is only a limited representation of the actual aquifer, particle tracking the Modpath way does guarantee proper distribution of the particles throughout the aquifer while maintaining the mass balance at any point as well as in the aquifer as a whole.

The procedure to follow is to first generate a conductivity field. Then use Modflow to compute the flow field in the aquifer, with heads and cell-by-cell discharges. This is allows by the computation of the stream function using the flow across the right face of the cells that were computed by Modflow. The next step is to place particles along a vertical in the aquifer at elevations obtained from the stream function, such that each particle represents the same amount of discharge along this vertical. After releasing the particles they are tracked with Modpath. Following step is to take the computed pathline file and for each particle compute when exactly it passed a set of given points in the aquifer. Finally we determine the cumulative breakthrough curve for each of these locations. These breakthrough curves represent the cumulative probability density function of the dispersion between the release point and the observation point, they capture the characteristic of the dispersion processes active between the two points. By using more points, the development of the cumulative density function over time or, rather distance, can be studied. These cumulative probability density functions can be converted into breakthrough histograms to unveil the underlying probability density functions. Both cumulative breakthrough curves and the histograms contain the same information.

3 Literature discussion

A vast number of papers has been written on subsurface transport of pollutants (Gelhar, Sudicky ...). This mainly started in the 1980s after it became obvious that hundreds of thousands of waste sites were and have been polluting groundwater and groundwater and as an available resource for drinking water and public concern skyrocketed. The study of the subsurface displacement and spreading proved difficult due to the heterogeneity of the subsurface and the interaction between pollutants and subsurface material. The studies were plagued by lack of understanding the complexity of the conductivity field that caused preferential flow paths and the mixing processes known as dispersion as well as the role of diffusion in it. The Fickian or Gaussian theory that look so nice on paper, or in math, was time and again challenged in practice, where samples showed that reality and theory more often than not did not match. Hence long time studies were undertaken with large-scale and repeated tracer tests to better capture and learn to predict what happens in practice. The Borden en Made studies, both done over 25 years with millions invested in exploring the subsurface structure and sampling the groundwater in great detail were carried out, but in the end did not totally solve our lack of insight and modeling capabilities to correctly predict development of pollution plumes in those and other circumstances.

Sudicky (1986) carefully studied the Borden experiment after others, like Dagan and Gelhar went before him. He gives a cross section in both the longitudinal and perpendicular direction to the groundwater flow. His paper is more or less a summarizing evaluation of the work that was done at Borden. Sudicky considers the flow as fundamentally 3D and finishes with a summary worth citing from it.

Zheng et al. (2011) provide a review and overview of over 25 years of research and lessons learned at the Macrodispersion Experiment (MADE) site, located at the Columbus Air Force Base in Mississippi. The site has been instrumental in advancing the understanding of solute transport in highly heterogeneous aquifers. The authors conclude: „In spite of tremendous effort and progress over the past three decades, our ability to predict solute transport processes in highly heterogeneous media remains very limited”. They show to expect

a lot from future field measurements in a comprehensive suite and carefully designed in a tightly integrated fashion. However, it's doubtful if these new studies will be ever performed, given the effort and cost already spent before. It seems that the existing data for the Made and Borden will be revisited in new research for a long time into the future. The authors stress that future work should focus on mapping the hydraulic conductivity distribution and the resulting preferential pathways far beyond what is currently possible given the existing measurement techniques. With this disclaimer the authors seem to admit that the problem to fully understand subsurface transport will remain essentially unsolved for a long time in the future.

Gorelick has essentially introduced the dual domain theory and model to better capture the observed dispersion at the very heterogeneous Made site ([[Zheng et al. \(2011\)](#)]). The dual domain was then included in several groundwater transport codes, like MT3SM. The dual domain just discerns between a mobile phase and an immobile phase, with kinetic exchange process between them. It has been quite successful in Made as is shown in figure 9 in [[Zheng et al. \(2011\)](#)]. It thus seems that a dual domain can compensate for the failure to accurately capture the hydraulic conductivity field to mimic the transport behavior with preferential flow paths. However, it may well be that the dual-domain model functions well for the wrong reasons by being able to produce a subsurface mass transport that mimics the measurements even if in reality there are not two domains but there is just a very heterogeneous conductivity field. The authors seem to admit this in their introduction stating that „results from field investigations and modeling analyses suggest that connected networks of small-scale preferential flow paths and relative flow barriers exert dominant control on solute transport processes.” These connected networks are fundamentally different from the adsorption process that is modeled by the dual domain seems to make no sense to model constituents that do not sorb like chloride, bromide or tritium. [[Fiori et al. \(2013\)](#)] show that indeed, it is possible to get similar outcomes with a heterogeneous conductivity field without a dual domain with sorption.

Two years after this review paper that should have said it all was picked up by [[Fiori et al. \(2013\)](#)]. They continued the discussion and tried to model the observed plume dispersion at the Made site. To better tackle the large asymmetry of the pollution plume not described by traditional advection-dispersion models, they propose a multi-indicator model (MIM). With it [[Fiori et al. \(2013\)](#)] essentially subdivide the aquifer into blocks of different independent conductivity drawn from a lognormal distribution. The dispersion generated by the flow of particles through their heterogeneous model was the result of advection alone. They found that this simple advection model could describe the development of the observed plume „remarkably well”. In their section 3, the authors explicitly motivate their claim that advection is the only process that matters at the Made site. With the few parameters given in their table 1, and used below in this report, their MIM model was capable of mimicking the measured bromide distribution sampled at 6 points of time, but only reasonably. Nevertheless, their MIM model did demonstrate that the observed dispersion can be explained just by the flow as it is distorted by the heterogeneity of the conductivity field in the aquifer, even without considering any other processes. The results of this advection-dominated model show the characteristic that proved impossible to model with traditional advecton-dispersion models, which is the large asymmetry (long tail) of the plume development in the subsurface.

The more homogeneous the conductivity field of the aquifer is, the less dominant is the spread of particles caused by advection and the more important diffusion and pore-scale velocity differences will be. Even then these low-scale velocity differences will dominate diffusion, at least in the flow direction. For instance, [[Jensen et al. \(1993\)](#)] show that, even though their Danish aquifer is very homogeneous, the derived longitudinal dispersivity was 500 times larger than the transverse dispersivity and 1000 times larger than the vertical transverse dispersivity. From this, we may conclude that velocity variations caused by local small scale conductivity variations are likely the cause of the large contrast between the vertical and transverse dispersivities. [[Jensen et al. \(1993\)](#)] proved this by showing that increasing refinement of their model better mimicked the small-scale statistics of the aquifer.

[[Jankovic et al. \(2006\)](#)] show that, even though macrodispersion can be described by velocity variations caused by the conductivity field, and result in largely asymmetric plume shapes with a short front and a long tail, the bulk of the plume can still be described by a Gaussian model with an equivalent mean velocity and a longitudinal dispersivity. This does not work for the long tail, but the tail will be of far less importance in practice as it only holds a small fraction of the total mass of the pollutant. Only when the aquifer tends to homogeneity, the Gaussian model will also better predict the plume's tail behavior. [[Jankovic et al. \(2006\)](#)] further concluded from their work, that for very inhomogeneous aquifers, the plume behavior does not approach Gaussian / Fickian behavior even for very long travel distances.

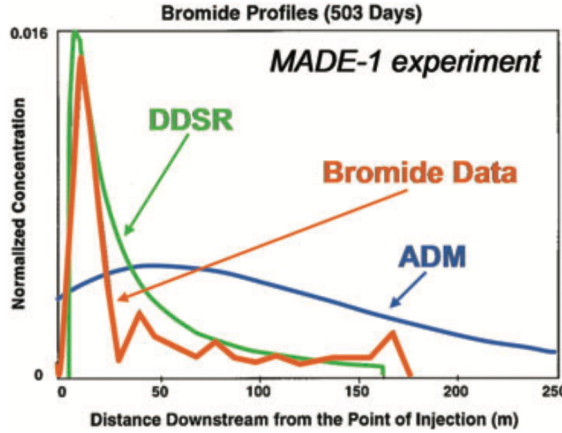


Figure 1: Comparison of the modelled and measured bromide plume extent at the Made site. ADM stands for classical Advection-Dispersion-Mass transfer model, DDSR stands for Dual-Domain Mass Transform Model. The graph clearly shows the rapid progress of a small part of the water while the bulk remain near the source. The interpretation depends on whether the flow rate hat the sampling elevations was included in the analysis. This is probably not the case.

4 Cross sections

4.1 Introduction

A fundamental problem, perhaps the most fundamental one, is that the flow in a 2D cross section misses the third dimension. The problem is not that some cross section is bended to follow the curves of a projected streamline, nor that the cross section represents an axially symmetric situation. The essence is that a plain cross section does not have flow components perpendicular to it. In theory a 2D section does not require flow components perpendicular to it; in practice, this is never fully the case. Wherever the flow and the spread of particles is determined by inhomogeneities, or, in other words, by the heterogeneous conductivity field, due to which the flow direction continuously deviates from the average flow direction in the cross section, one can then be certain that in reality such deviations also occur perpendicular to the 2D plane of the cross section. The inhomogeneities of the real world are never limited to the plane of the cross section, they are just as strong perpendicular to it. [Hemker and Bakker (2004)] and others have shown, that exactly this 3rd component of the groundwater velocity makes that streamlines can cross each other, and thus cause dispersion, what they never can in a 2D situation. The analysis of the flow in a flat cross section falls fundamentally short to describe the full mixing process in an aquifer characterized by its heterogeneous conductivity field in all its 3 dimensions. The paper of [Hemker and Bakker (2004)] triggered 3D thinking and made crystal clear the likelihood, or perhaps even the certainty, that a 3D inhomogeneous conductivity field will let streamlines cross each other all the time and everywhere, and thus cause mixing at a scale much larger than that at which molecular diffusion or pore-scale velocity differences play.

And of course particles (molecules) will jump between adjacent streamlines all the time, which, combined by the turnover of streamlines described above, triggers transversal spreading at a rate that far exceeds that of molecular diffusion. Molecular diffusion tends to be slow and becomes increasingly slower over time as expressed by the formula for the grow of the standard deviation of an initially sharp front, i.e. $\sigma = \sqrt{2Dt}$. However, in a porous medium like an aquifer, in which the velocity varies perpendicular to the stream lines everywhere, the concentration gradient perpendicular to the streamlines is kept much sharper. This is a consequence of the washing process associated with particles on adjacent streamlines having different velocities. This washing process cause molecular spreading to be larger than in the theory valid for a stagnant groundwater.

Finally, it is virtually impossible to determine particle concentration at distinct points in the aquifer. We do not get around the fact what we will always mix water from different streamlines when sampling,

no matter how we do this. This is true for even the smallest sampling screen, for a sampling well and for measuring concentration using some physical device, for instance by measuring electric conductivity or tracer color. If we consider advection to be the dominant or even the only relevant process taking place in the aquifer, then mixing will only take place at the moment we sample or extract. The best we can hope for is the sampling of the passage of a complete front.

To this we must add the the difference between sampling *in situ* without disturbing flow, for instance by a sounding device, or by extracting using for instance a well. Both methods will often given completely different results as the extraction method mixes the incoming water in proportions proportional to the conductivity along the screen, with some parts yielding most and other parts yielding least water, while sampling *in situ* measures without considering the amount of flow that its elevation. Mixing these sampling methods can lead to misinterpretations

In conclusion if we ever want to model groundwater mixing appropriately, we must consider 3D velocity components, even when dealing with flat cross sections. When sampling we must realize the mixing we cause or not cause depending on the sampling method as the results may be completely different.

In the analysis for this work, we will at least initially focus on the flow in vertical cross sections without any flow perpendicular to them and should be aware of its limitations.

4.2 Generating cross sections

For any analysis we need a conductivity field first. There are many ways to generate cross sections. One manner is to do this based on a colored picture, by sampling the pixel colors, clustering these colors, and then assigning distinct conductivities to each of them. Although doable, and allowing many pictured cross sections to be used in this way, the resulting sections will always be artificial as no single hand-made image of a cross section can ever grab, even nearly, the real-world conductivity variations that are present in reality. These cross-section pictures have too few colors, and on top of this, the colors tend to picture perceived facies or formations rather than conductivities.

Cross sections may also be obtained from websites that provide them based on borelogs and other physical logs, cores etcetera. Such geological sections are exactly those meant above. However, sites such as Dinoloket.nl provides a full 3D database of the likelihood of the occurrence of a set of materials (sand, clay etc.) for blocks (voxels) of some 100x100x0.5 m across a large part of the Netherlands. It is straightforward to extract colored cross sections form this website and use them in the way described above. However, these data are also very limited in that the number of voxels is much larger than the resolution of the underlying data, so that they do not represent reality, but instead, the probability of the occurrence of given materials, which can then be associated with conductivities. If we associate one conductivity with each voxel, then the result is likely too coarse to accurately simulate subsurface transport as caused by the more local heterogeneous conductivity field.

One can digitally generate boreholes by using transition probabilities between adjacent materials as obtained from borehole sampling. The resulting borehole is clearly artificial, but it will at least have some statistical properties similar to that of the real borehole. The problem then becomes how to link manyi n this way created boreholes together into a single cross section. Simple interpolation will not be enough as it then ignores the horizontal transitions or at least the scale of them. And it is not clear how to solve this issue without external information, which, in fact, cannot come from boreholes drilled at mutual distances in the order of hundreds to thousands of meters. Such information could come from the study of existing real-world cross sections for similar sedimentological environments. It is likely that the number of real-world cross sections that actually match the sedimentological environment in the subsurface in which we drill our boreholes, is far too small to yield accurate data.

From such cross sections rather than from individual boreholes that are too far apart, we can extract the statistics of the grainsizes or even the hydraulic conductivity in the horizontal and vertical direction by constructing semi-variograms. Then use these to statistically generate individual cross sections, also know as realisations, which at least have this same statistical properties as the real cross section. The problem is, that each realization is different and no one will mimic the actual field situation accurately. The only thing we can then do, is generate a large number of such realisations and study the properties for the ensemble, the results of which are always statistical themselves.

Finally, we can just generate our 2D cross sections, or even complete 3D conductivity fields digitally

be sampling from conductivity distributions in some way ([[Fiori et al. \(2013\)](#)]) or by placing distinct heterogeneities in a 2D or 3D field ([[Jankovic et al. \(2003\)](#), [Jankovic et al. \(2006\)](#), [Jankovic et al. \(2010\)](#)]), of which the link to reality will remain unanswered.

4.3 Cross section according to De Lange

in his papers, takes an approach that is similar to that of [[Fiori et al. \(2013\)](#)] et al. He divides his vertical cross sections for the sake of dispersion simulation into blocks, which he calls domains. These blocks have a background conductivity with one embedded elongated facies with a conductivity that is largely distinct from the block's background value. The entire dispersion process takes place inside the block. To simulate a long travel distance, many alike blocks are placed next to each other and on top of each other, thus filling the entire space of the vertical cross section.

We can also just fill the entire cross section with blocks of the same size, each of which has it's own distinct conductivity drawn from a statistical, i.e. lognormal distribution. The cross section will then be similar to the model domain used by [[Fiori et al. \(2013\)](#)] at al.

4.4 More elaborate cross sections

A next step to more realism is to make sure that not only the probability of encountering certain conductivity values matches that in the real aquifer, while also honouring their spatial covariance or their horizontal and vertical transition probability. This should better mimic the extent of the heterogeneities at the scale of the layers in the aquifer and the horizontal structure that we observe in actual geological cross sections. In fact, doing this, will satisfy the statistics of the real cross section as while keeping it's character determined by adjacent distinct facies, but the aquifer may look completely different than the real one. It's just a computation object required by our model.

4.5 Going fully geostatistical

Going fully geostatistical would be a final step towards more realistic simulations. However, simple semi-variograms of the distribution of conductivities will not be enough; generating cross sections from it would smear out the distinct boundaries between facies. Hence, going fully geostatistical will require advanced geostatistical methods to allow honouring all features that we observe in real-world cross sections.

4.6 Finally still lacking the third dimension

Even if we go fully geostatistical to maximize the match between our digital and real-world cross section, we still miss the third dimension, which may prove essential for mixing by the likely ubiquitous 3D cross-over of streamlines with associated particle exchange. This simply implies that we either include the third dimension in our cross section or we mimic its effects by introducing some vertical mixing process that mimics it, like vertical dispersion. It's importance may vary though, but totally excluding it may prove wrong, especially in high-conductance zones.

5 Cross section simulations

5.1 Basic properties

Because high-conductive facies of some horizontal extent seem to matter most for the observed pollutant breakthrough curves, our cross section must reflect this. There are different ways to generate sections with such properties. The one we adopt here is inspired by [[Fiori et al. \(2013\)](#)], [[De Lange \(2020\)](#)] and the sedimentological origin of them as explained in [[Coe \(2003\)](#)].

A rectangular array of conductivity zones is created. Then a cell in the array is arbitrarily chosen to center the next zone. The height and width of the zone are then chosen to label the area of the overall conductivity array. This is done until all cells of the conductivity array have been labeled. As a last step,

the conductivities are randomly selected from a log-normal distribution and associated with each of the labels to generate the final conductivity field.

The conductivity field was generated using the data of [Fiori et al. (2013)], table 1.

$$K_G = 8.9 \times 10^{-6} \text{ Geometric mean of } K \text{ [m/s]}$$

$$\sigma_y^2 = 6.6 \text{ Logconductivity variance}$$

$$I = 10.2 \text{ m Horizontal integration scale (range of the semi-variogram of } k_k)$$

$$I_v = 1.5 \text{ m Vertical integration scale (range of the semi-variogram of } k_v)$$

$$\theta = 0.31 \text{ Porosity}$$

$$J = 0.0036 \text{ Mean head gradient}$$

I did not use the parameters I and I_v directly.

5.2 Made cross section as applied by Fiori et al (2012)

Because of their success, we will mimic the the construction of cross sections used by [Fiori et al. (2013)] in their MIM (multi-indicator) model to simulate plume break-through at the Made site. These sections consists of cubic blocks of equal size, equal to $2R$.

$Y = \ln(K)$ is normal with $\text{mean}(Y) = \ln(K_G)$ and variance σ_Y^2 and of stationary symmetric autocorrelation $\rho(r')$ where $r' = \sqrt{\left(\frac{r_x^2 + r_y^2}{I^2} + \frac{r_z^2}{I_v^2}\right)}$

The conductivity field in figure 2 has been generated as an exponential random field according to the parameters used by [Fiori et al. (2013)].

$$C_h = C_0 \left(1 - e^{-\frac{h}{I_h}}\right); \quad C_v = C_0 \left(1 - e^{-\frac{h}{I_v}}\right)$$

These parameters are in the header of the figure. The zones all have the same width, equal to $2I_h = 21\text{m}$. The field was first generated with gstoools using an exponential model with lengths equals to I_h and I_v using the values for the mean conductivity and the variance of its logarithm as given in the figure 2. Next the section was divided into blocks of width $2I_h$ and the conductivity value generated at its center was attributed to the entire block. The blocks on overlying layers are shifted relative to each other as was done by [Fiori et al. (2013)].

The k -field was then used in Modflow to compute the heads and flows with fixed-head boundaries at both ends such that the mean head gradient was $J = 0.0036$. The Modflow results permit computing the stream function, which is given in figure 3. No particle tracking is needed for that. The stream lines, which are the contour lines of the stream function, clearly show how the particles flow up and down through the aquifer as caused by the heterogeneous conductivity field. From these vertical components it should become immediately clear that there must also be components perpendicular to the cross section in real-world circumstances, which are neglected here but could be incorporated with a 3D model generated in the same way.

Figure 4 shows the pathlines as tracked by Modpath. 100 particles were released but only every 5th particle path is shown for clarity. The release elevations based on the stream function, are such that each particle represents the same amount of flow. The pathline pattern matches perfectly that of the streamlines, as they should in a steady-state situation. The heads are not shown here, but they are shown in figure 3.

Figure 5 shows the computed cumulative breakthrough curves at intervals of 100 m along the cross section. The times are quite long, which is due to the length of the section and the enforced gradient $J = 0.0036$. Notice the long tails for the greater x -values. Long tails are expected whenever the mass transport is essentially caused by advection through an aquifer that is heterogeneous on scales that are substantial with respect to the cross section. The size of the heterogeneities of $2I_h = 21 \text{ m}$ in this cross section can be observed in figure 2.

Finally, we compute the histograms from the obtained cumulative breakthrough curves. These overlapping histograms are shown in figure 6. The histogram for $x = 1000 \text{ m}$ clearly shows the asymmetry of the

density curve with its steep front and long tail, a phenomenon that is characteristic for advection-dominated transport through a heterogeneous subsurface. To better analyze the outcome, the breakthrough times curves have been fitted by the lognormal distribution as shown in figure 7. The lognormal distribution fits very well. Note that due to the skewness of the lognormal distribution, we have $t_{mode} < t_{median} < t_{mean}$, the values of which are also indicated in the figure. Instead of using the usual quantiles (0.05, ..., 0.95 of the cdf) to indicate the bulk and outliers, we used 0.2, 0.5, 1.0, 2.0 and 5.0 the $t_{mode} - t_0$ as more informative values. The pdfs are shown in the bottom figure and clearly demonstrate the skewness of the break-through times.

Figure 8 shows the position of the particles at given observation times. These particle positions were ordered and fitted by the lognormal distribution, of which the cdf is shown together with the outcomes of the simulation. The fit is less good than that for the break-through times. The obvious reason for this is that for the times, every particle has passed the entire 1000 m length of the model, where for the positions of any given observation times this is at all the case. Therefore, particles that traveled little at a given time, have seen only a small part of the model's heterogeneity and are thus subject to more randomness. The latter may only be solved by repeated realizations and taking the ensemble at the end. The graphs with the particle positions seem to more resemble the normal distribution than those for the break-through times. However, this may especially be the case for larger observation times. The graphs with the particle positions also make clear, that a portion of the particles hardly moves at all, which is indicative of tail formation. One is tempted to compare the pdf with the particle position with the data for the Made site as shown in figure 1. There the mode at $t = 503$ d was at about 15 m from the source; in figure 8 bottom at $t = 600$ d it's at about 20 days, which is not too different. Note that in this model the same aquifer and gradient values were used as published for the test at the made site ([[Fiori et al. \(2013\)](#)]). All in all, I don't see that the result by [[Fiori et al. \(2013\)](#)] is too convincing as a travel distance of the mode of 15 m is small with respect of their fixed box size of about 20 m, and therefore, really small with respect to the size of the heterogeneities in their model, implying that chance may play a big role at these outcomes.

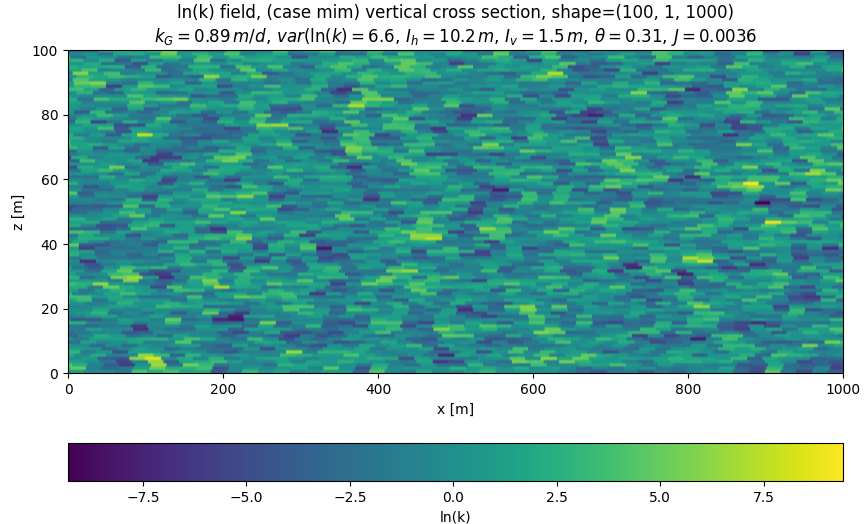


Figure 2: log- K -field, like in [[Fiori et al. \(2013\)](#)] with the same parameters (see header)

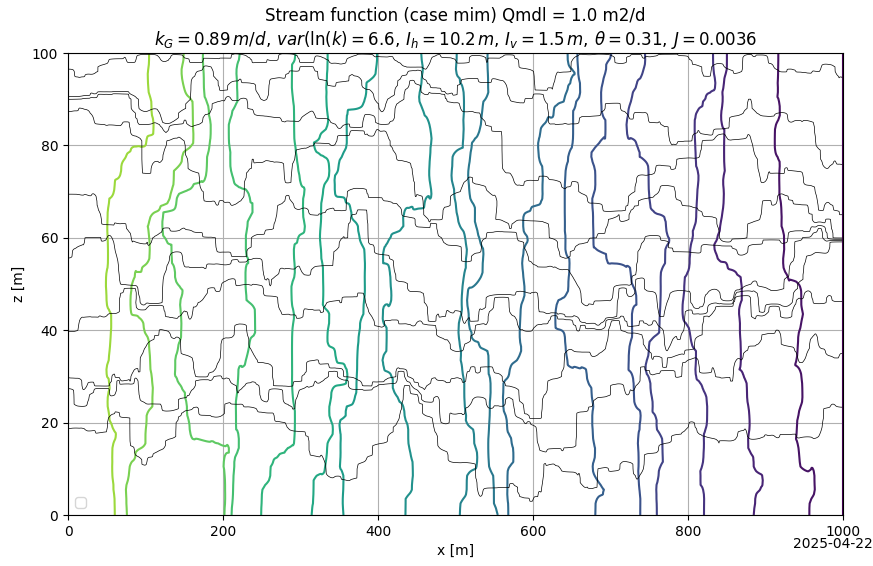


Figure 3: Stream function computed from the flow-right-faces in the cell-by-cell budget file generated by Modflow

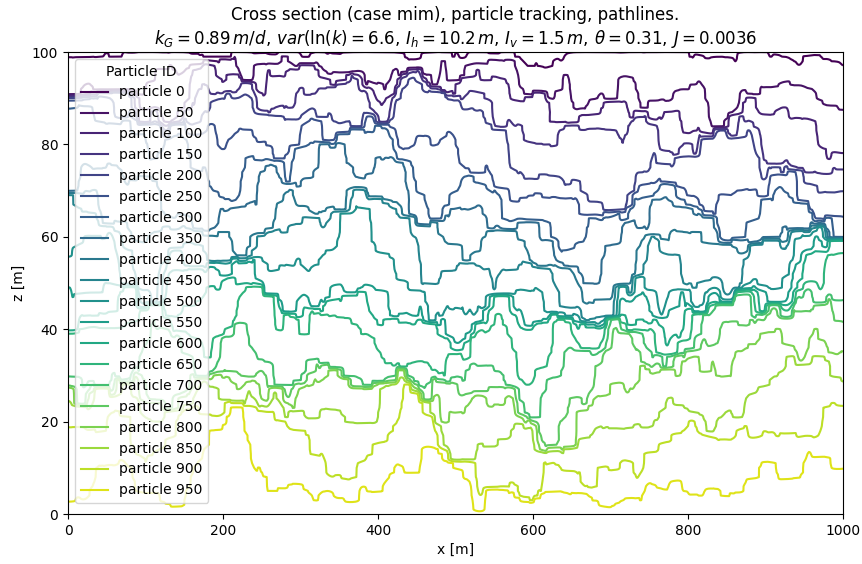


Figure 4: Modpath-computed pathlines.

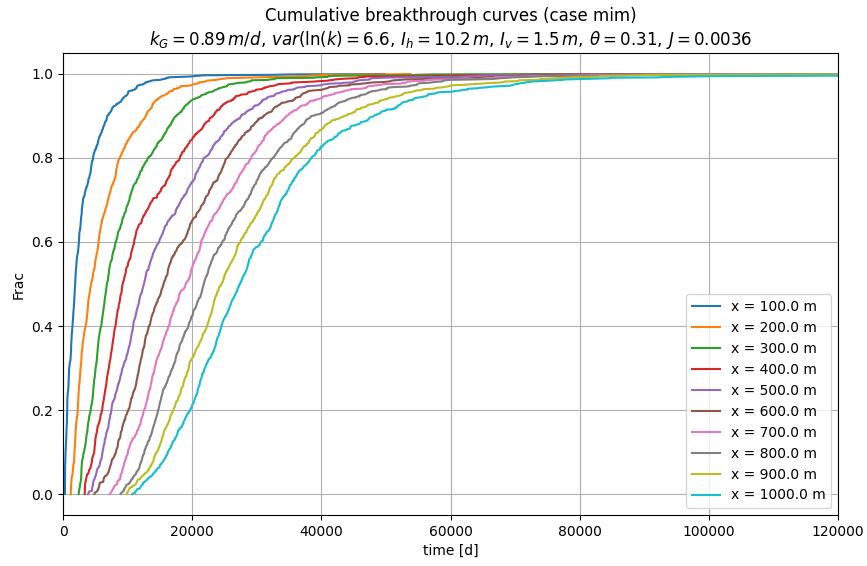


Figure 5: Computed cumulative break-through curves

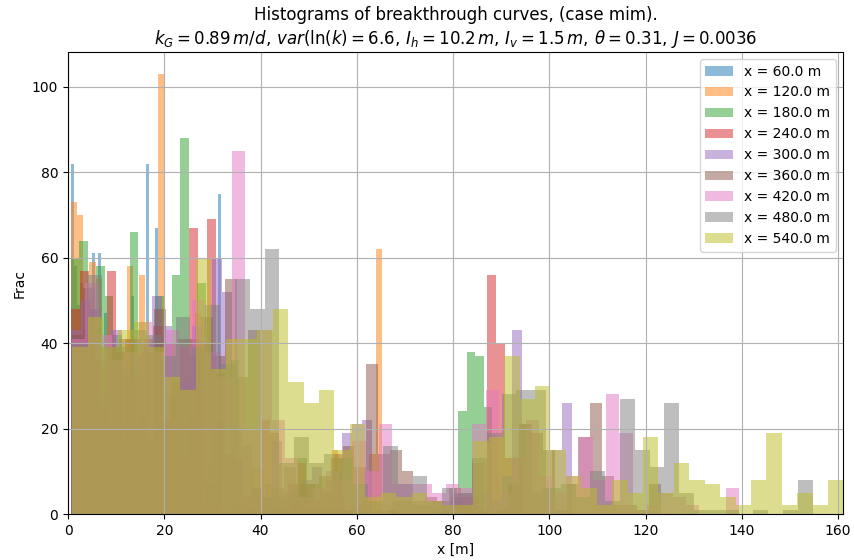


Figure 6: Computed break-through histograms

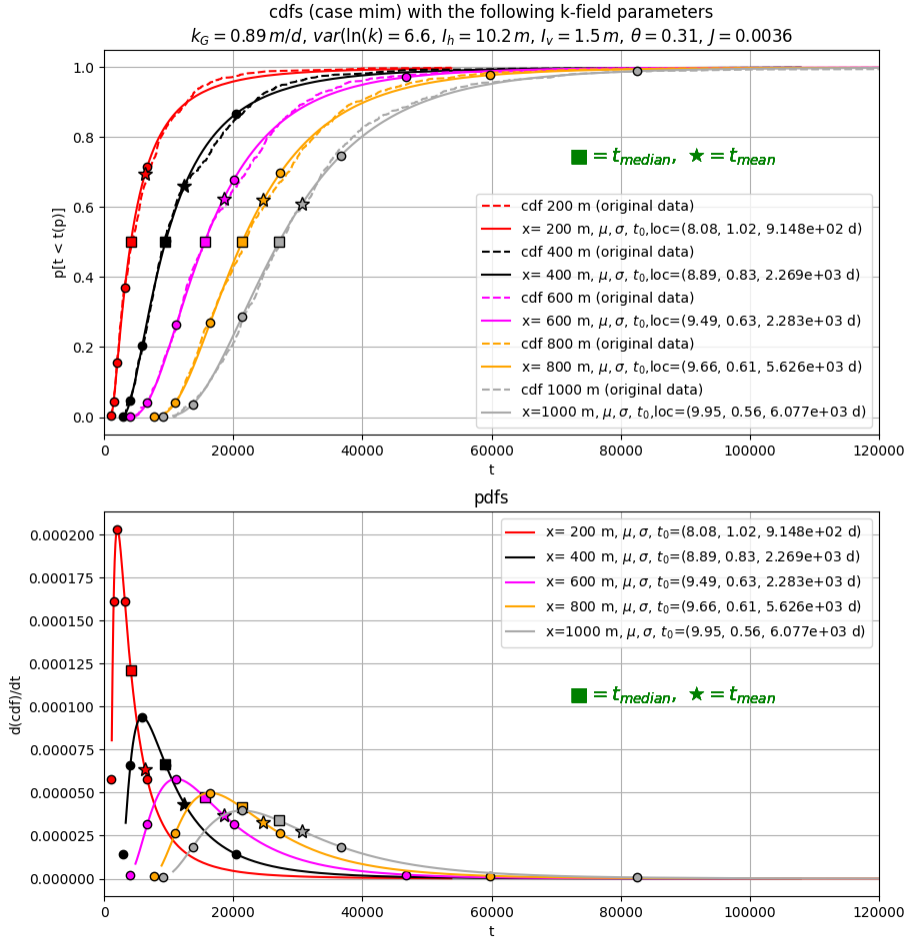


Figure 7: Top: Breakthrough curves with fitted cdf for lognormal distribution. Bottom their pdf. The median and the mean are given and the points at 0.2, 0.5, 1.0, 2 and 5 times $t_{\text{mode}} - t_0$ which provide a better insight with the lognormal distribution than the usual quantiles of the cdf. Because of the skewness, $t_{\text{mode}} < t_{\text{med}} < t_{\text{mean}}$. The skewed character of the breakthrough curves are clearly visible. The maximum time is about 5 times the minimum time in this case. The t_{mode} at $x_{\text{Obs}} = 200 \text{ m}$ is at about 400 d.

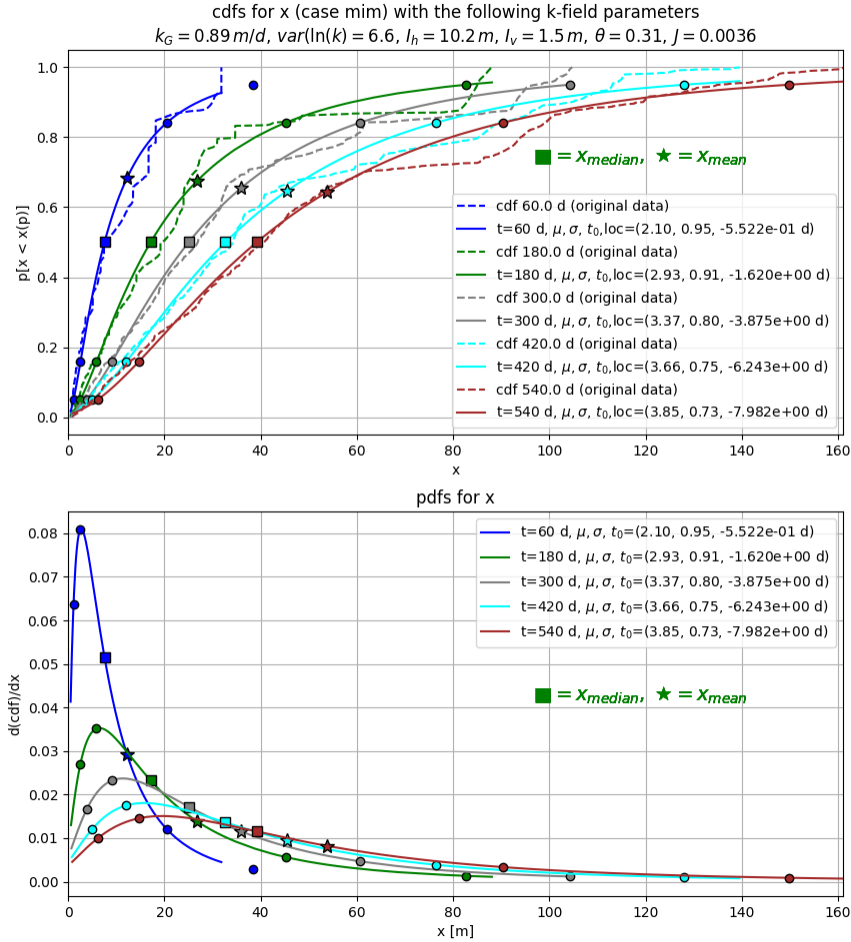


Figure 8: Top: Cumulative distribution of particles with their fitted cdf at given observation times. Bottom: Their pdf. Shown are x_{median} and x_{mean} . Notice that $x_{mod} < x_{median} < x_{mean}$ for the lognormal distribution. Also show are the points for $cdf = 0.05, 0.16, 0.5, 0.84$ and 0.95 . These work better than the mode-related values above as the distribution for the x -values is less skewed than for the t -values.

5.3 The same cross section with the same parameters except for a much lower variance of the conductivity, namely $var(\ln(k))$ is 1.1 instead of 6.6

The more homogeneous the aquifer, the more the breakthrough will conform to Fickian or Gaussian character with more symmetrical breakthrough curves and histograms. We can test this with the same model by just changing the variance of the $\ln(k)$ field from 6.6 in the previous case to 1.5, a value which I deem more realistic for the more homogeneous aquifers found in the Netherlands. The results are given in the figures below. Figure 9 looks similar to figure 2, however, the colorbar below it shows that the values are different, and less extreme. Figure 10 shows that although the streamlines still go up and down along their paths, these fluctuations are now much less than those in figure 3. Also, the head contours are much more straight in figure 10 than in figure 3. This is also due to the more homogeneous aquifer that we created in this section. As expected, the cumulative breakthrough curves now show much more symmetry about the 50% value, with far a less extreme tail. In fact, except for the small asymmetry in the last curve for $x = 1000$

m, asymmetry are essentially absent for all shorter travel distances. Hence, all breakthrough curves are now essentially Gaussian. The symmetry of the breakthrough behavior is also revealed by the histograms and jumps into the eye when comparing figure 13 with figure 6.

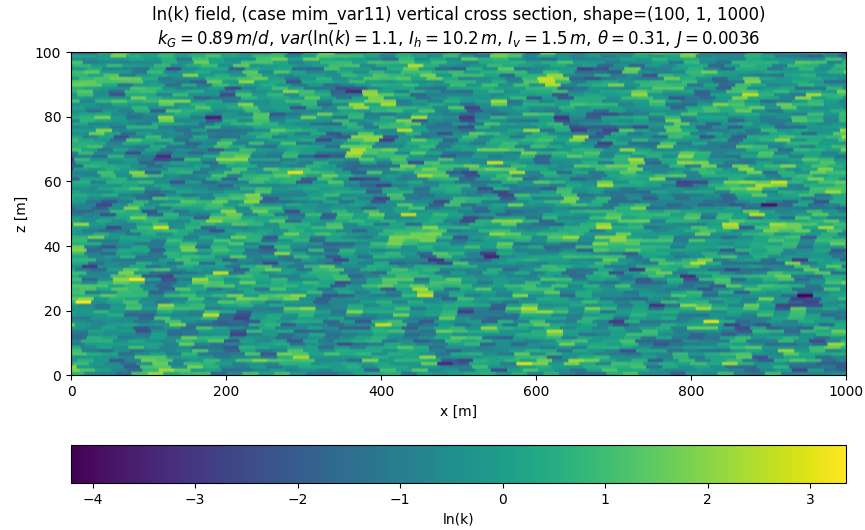


Figure 9: Image of the generated $\ln(k)$ field for the cross section. For the rest the parameters are the same as in the previous section

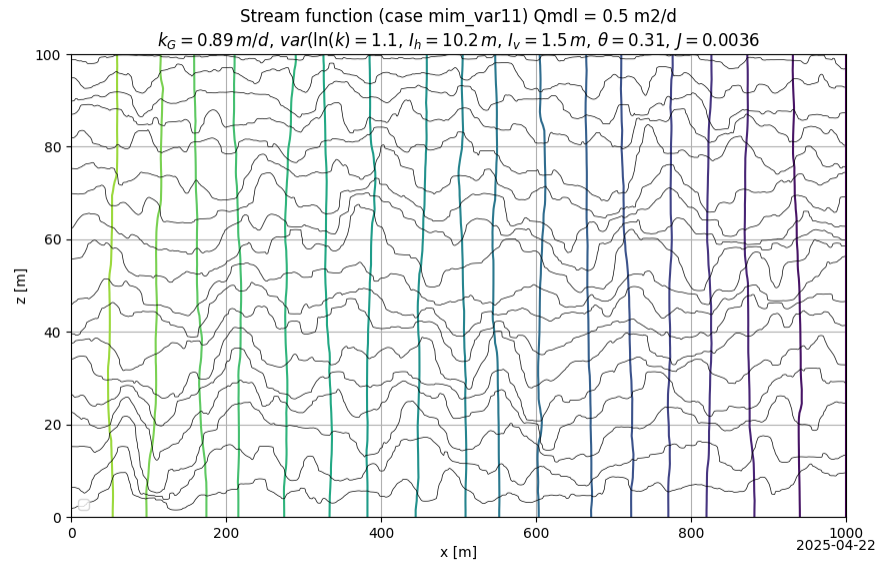


Figure 10: Streamlines and head contours of the cross section computed using Modflow.

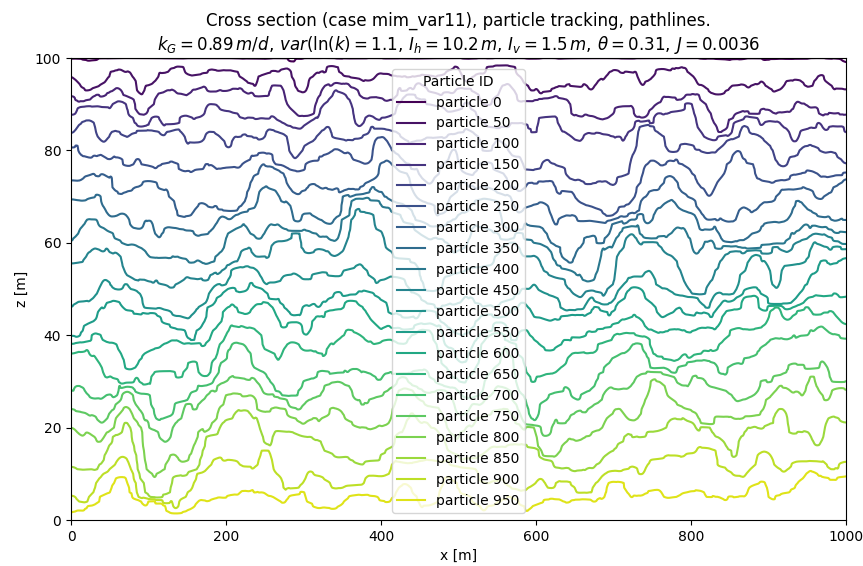


Figure 11: Pathlines, only every 5th particle is shown

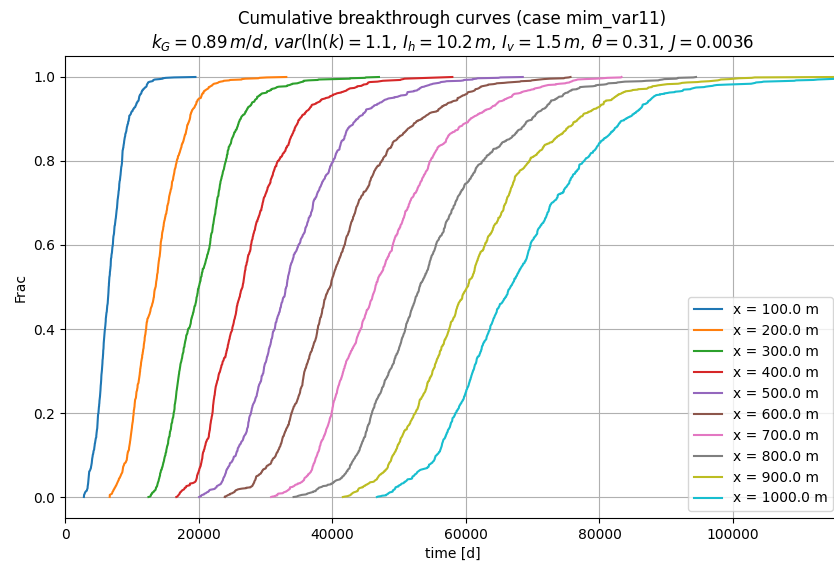


Figure 12: Cumulative break-through curves for different locations in the cross section

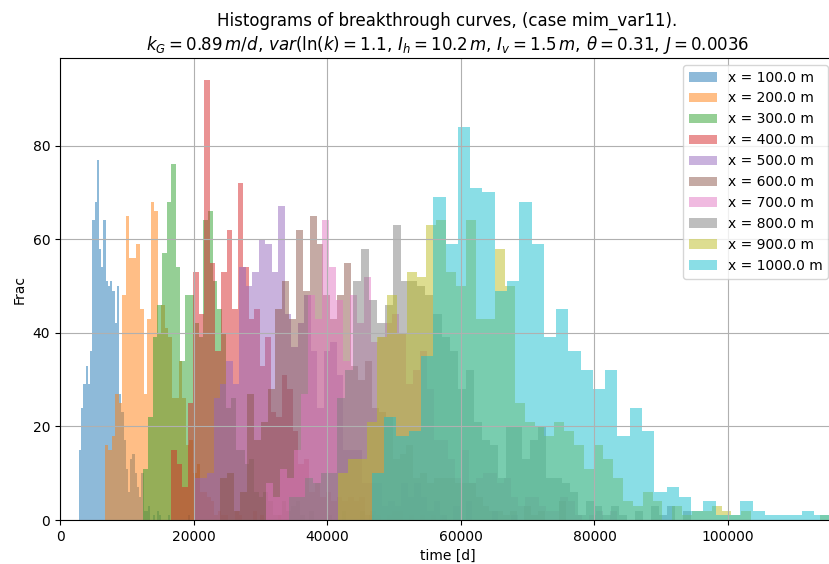


Figure 13: Histograms for the break-through at different locations long the cross section as computed from the cumulatives.

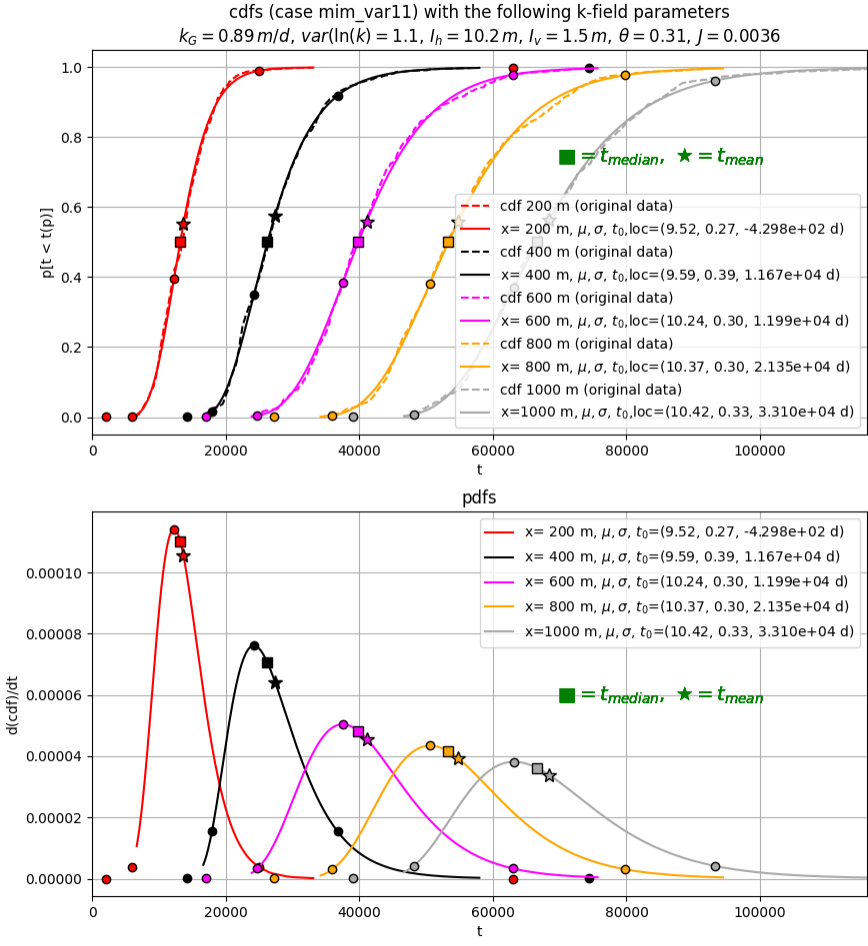


Figure 14: Top: Breakthrough times and fitted log-normal cdfs for same case as before by $\text{var}(\ln(k)) = 1.2$ instead of 6.6. Bottom: pdfs. Note the dots are at circles are at $t_0 + f(t_{mode} - t_0)$ with $f = 0.2, 0.5, 1.0, 2.0, 5.0$, where t_0 is the lowest possible value for the lognormal distribution ($t_0 = loc$) where loc is one of the parameters given by the fitting of the computed data. These points are here less insightful because the distributions are far less skewed than in the previous case with the much larger $\text{var}(\ln(k))$ value of 6.6 instead of 1.1. The maximum time is about 3 times the minimum time in this case. t_{mode} at $x_{Obs} = 200$ m is about 15000 days, which is about 4 times later than in the previous case. Also the mean time is larger now. At $x_{Obs} = 1000$ m it is now about 75000 days while in the previous case it was about 38000 days, shorter due to higher conductivities in the longest heterogeneities.

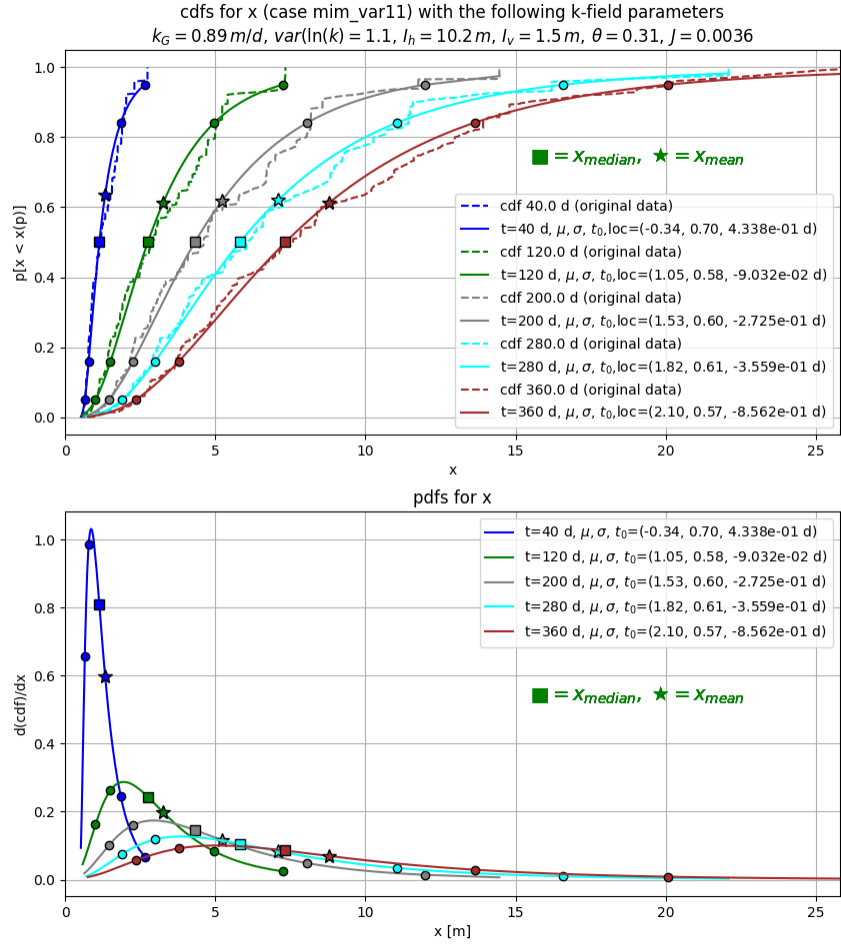


Figure 15: Top: Cumulative location curves from the model and fitted cdfs.. Bottom: companying pdfs. Circles are for $cdf = 0.05, 0.16, 0.5, 0.84, 0.95$.

5.4 Regular conductivity field as exponential random field with the same parameters as used in the MIM model of section 5.2.

The MIM model to simulate the MADE breakthrough curves in [Fiori et al. (2013)] uses blocks of width $2R$, essentially $2I_h$ with each having a constant conductivity throughout the block, while these block conductivities area conform the statistics for $\ln(k)$, for $\text{var}(\ln(k))$ and for the integration lengths I_h and I_v . Instead of using blocks, it may be feasible to simply generate a cross-section that fulfills these conditions but without resorting to the blocks of the MIM model. The cross section generated this way, is shown in figure 16. It lacks the block structure, which characterizes the cross section of figure 2. The stream and head lines in figure 17 are as irregular as in figure 3, which is due to the same large log-conductivity variance used in these two cases. Figure 18 shows the breakthrough curves. The top figure shown those belonging to the current conductivity field, while, for easy comparison, the bottom figure is the same as figure 5 for the model with the block structure, but otherwise the same parameters. Figure 18 makes clear that, also with a fully continuous random field with exponential covariance, similar breakthrough curves are obtained as with a MIM-type model with blocks. Probably it is just the applied range of the horizontal and vertical

variograms that matter to get a behavior characteristic of preferential flow path, while it does matter little if a block structure is added. Figure 19, on top, shows the histograms derived from the breakthrough curves for this continuous cross section, and at the bottom, again for easy comparison, those obtained with the block structure and otherwise the same parameters already shown in figure 6. I would argue that both figures are not too different. They are essentially characterized by asymmetry with a large tail, which is what one expects from a strongly heterogeneous aquifer.

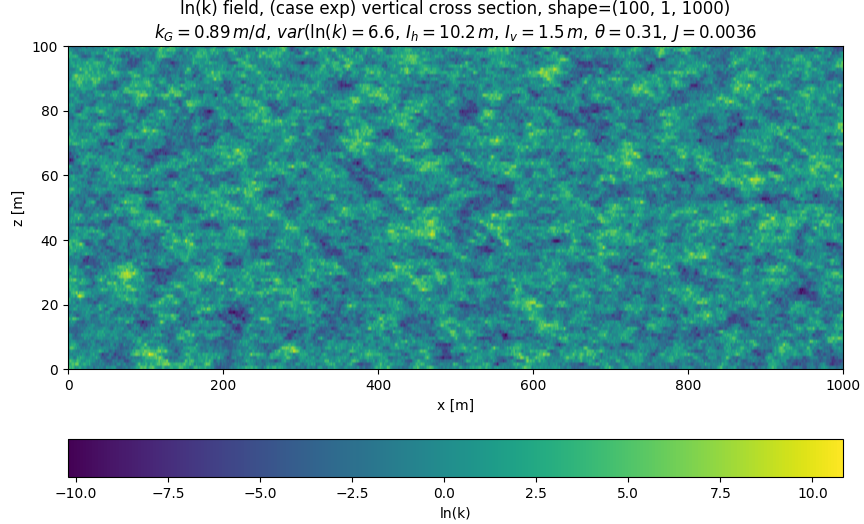


Figure 16: Generated $\ln(k)$ field using exponential model with variance and $x_{len} = I_h$ and $z_{len} = I_v$, and the parameters given in the header of the figure.

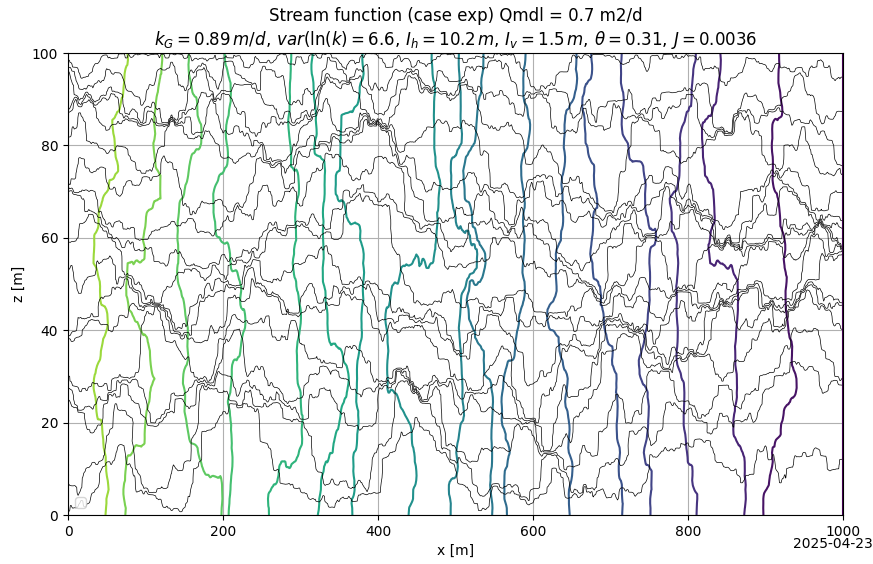
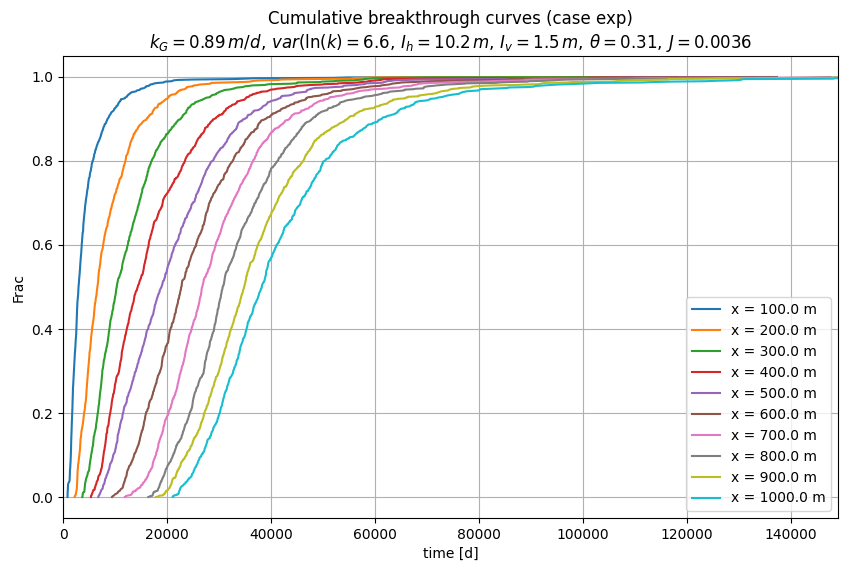


Figure 17: Stream function and head contours after simulating the cross section with the conductivity field in the previous figure.

Exponential random field field



MIM blocks field (using the same exponential field parameters)

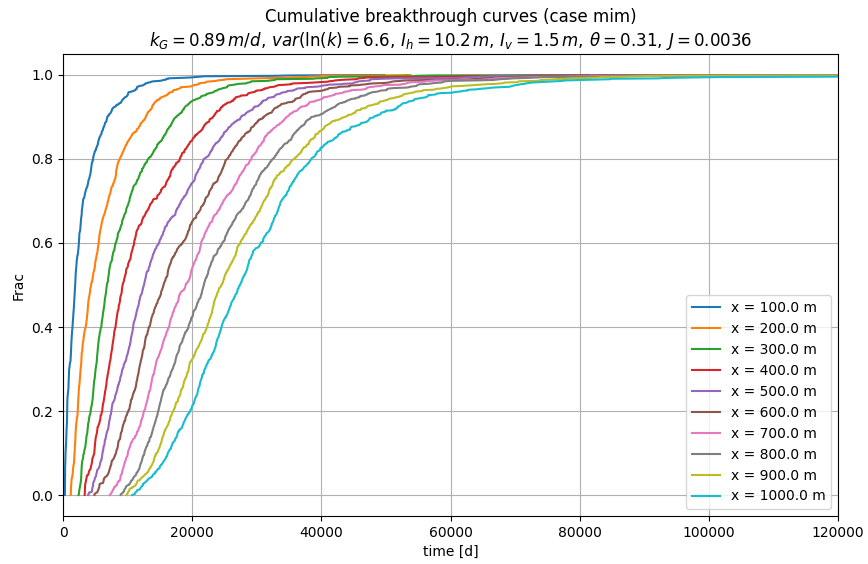
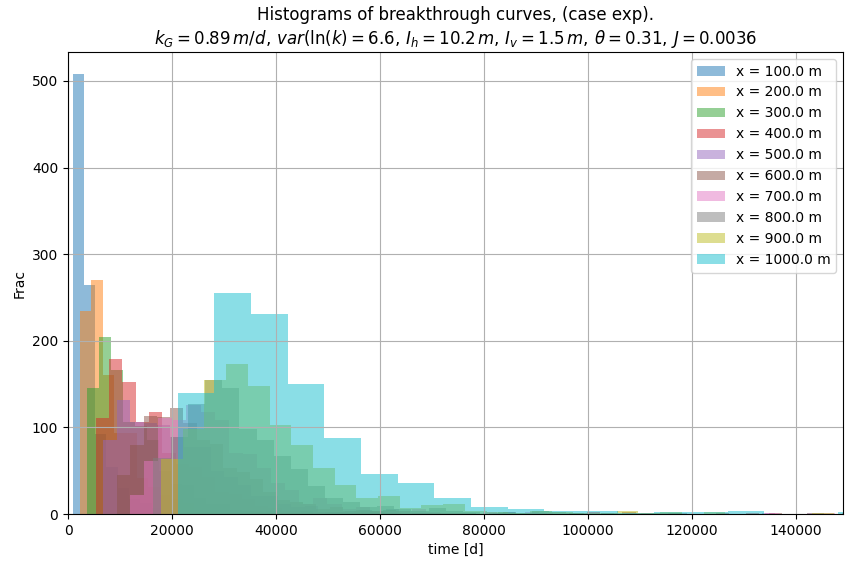


Figure 18: Breakthrough curves compute using Modpath.

Exponential random field



MIM block field with the same exponential random field parameters

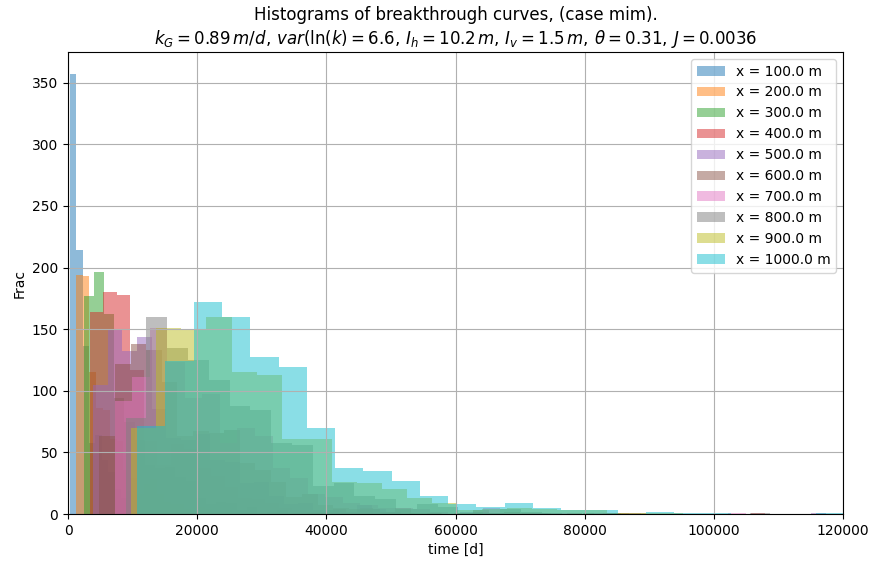


Figure 19: Histograms derived from the breakthrough curves in figure 18

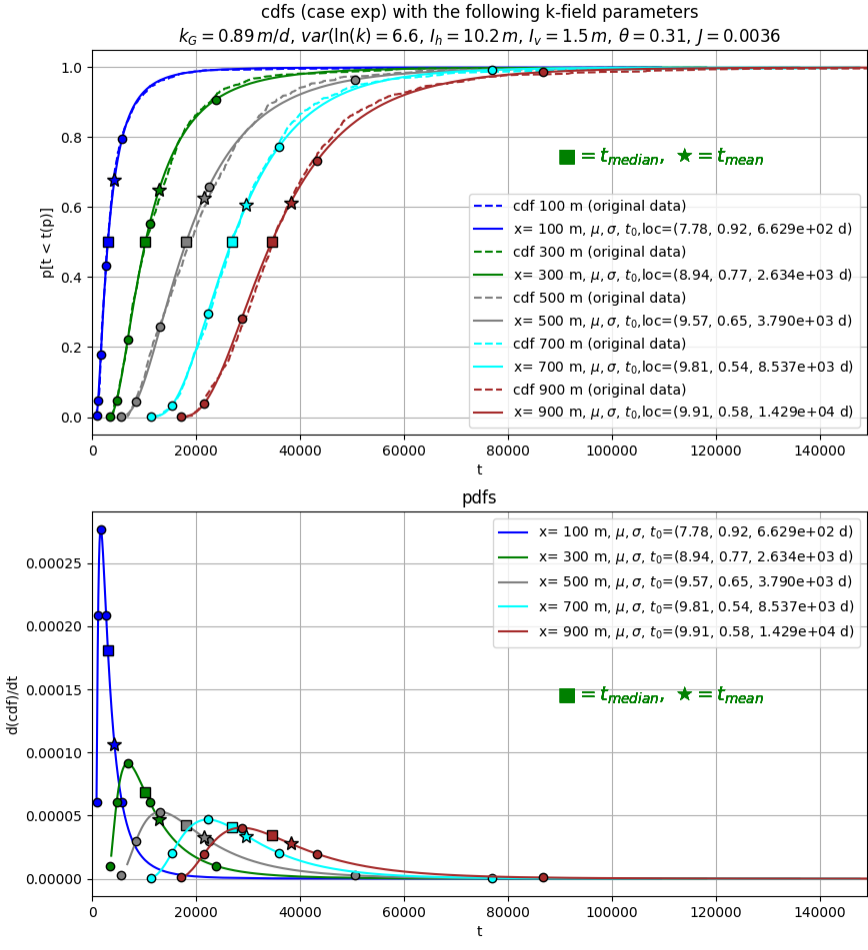


Figure 20: Top: Breakthrough curves and fitted lognormal cdfs. Bottom: pdfs of the same distributions. Circles are at $t_0 + f(t_{\text{mode}} - t_0)$ with $f = 0.2, 0.5, 1.0, 2.0, 5.0$, where t_0 is the lowest possible value for the lognormal distribution ($t_0 = \text{loc}$) where loc is one of the parameters given by the fitting of the computed data.

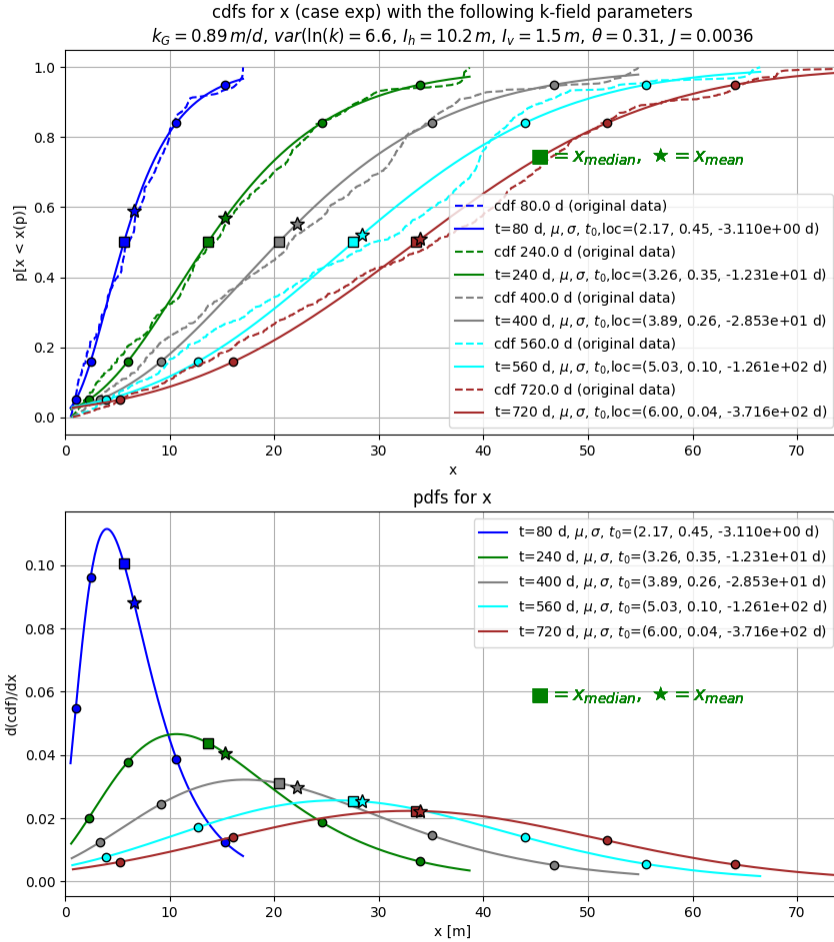


Figure 21: Top: Cumulative location curves from the model and fitted cdfs. Bottom: companying pdfs. Circles are for $cdf = 0.05, 0.16, 0.5, 0.84, 0.95$

5.5 A purely random field

The next example is for a purely random conductivity field in which the value for each model cell is sampled from the lognormal distribution with given k_G and $\text{var}(\ln k)$ as stated in the header of the following figures. The idea is that a purely random field has no preferential paths. It should, therefore, generate breakthrough curves that resemble the normal distribution, with symmetrical head and tail.

Figure 22 and figure 23 clearly show that the field is not purely random. The breakthrough curves in figure 24 indicate the symmetrical character of the breakthrough curves, which leads to almost normal pdfs in bottom image if figure 24. Figure 26 show the location breakthrough curves for different observation times as obtained from the same pathline computation. These too tend to symmetry with respect to the average particle location over time. The analysis in figure 26 confirm this. Note that the more t_{mean} and t_{med} tend to t_{mode} the more the distribution resembles the normal distribution. This is very close in this case with a purely random conductivity field.

As expected from the theory, the asymmetry with the time-breakthrough curves and their pdfs is much less in this case with purely random conductivity than in the previous case with a large horizontal integration

length, which generates a tendency to develop preferential pathlines. However with respect to the location breakthrough curves and their pdfs for different observation times, this is much less the case. These curves are actually very symmetrical in both cases. This is just an observation without being clear what the underlying theory would look like, which predicts breakthrough curves at different observation distances that are far more asymmetrical than the location curves for different observation times.

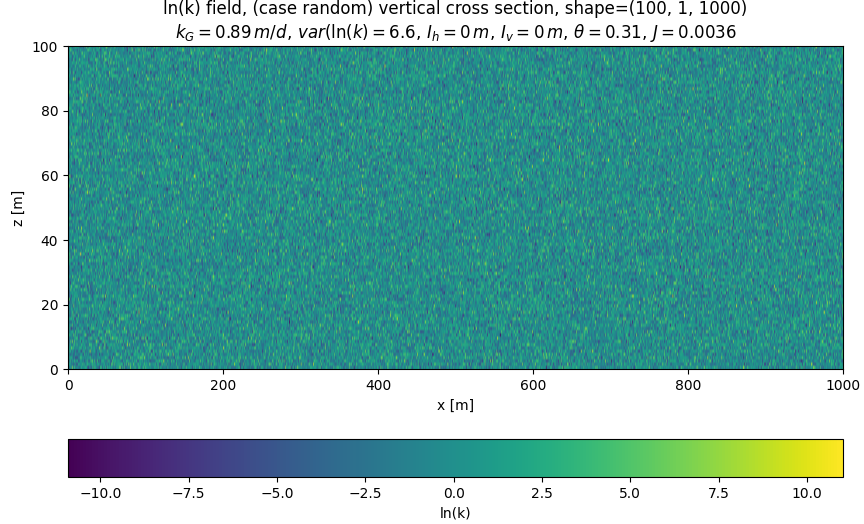


Figure 22: Random $\ln k$ field. Note the parameters in the header, which tell that the integration lengths are both zero in this case.

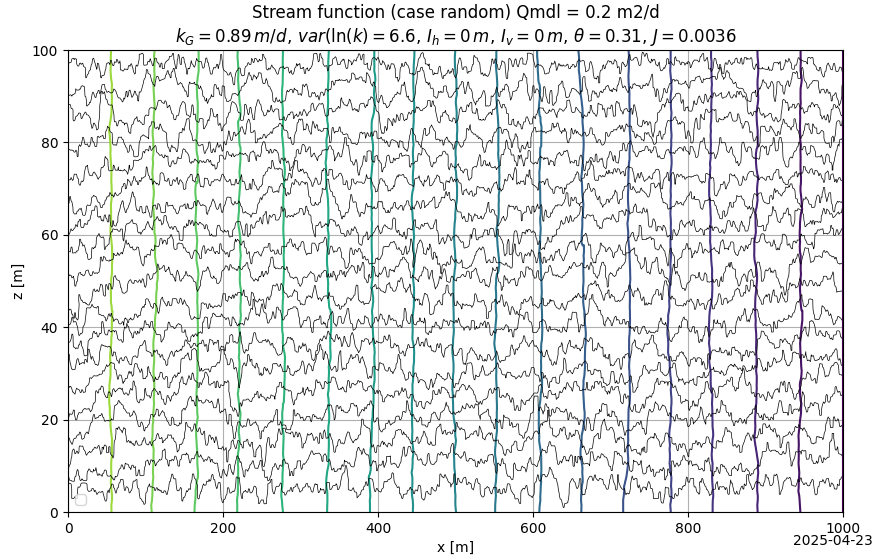


Figure 23: Stream function for random conductivity field. Same as pathlines.

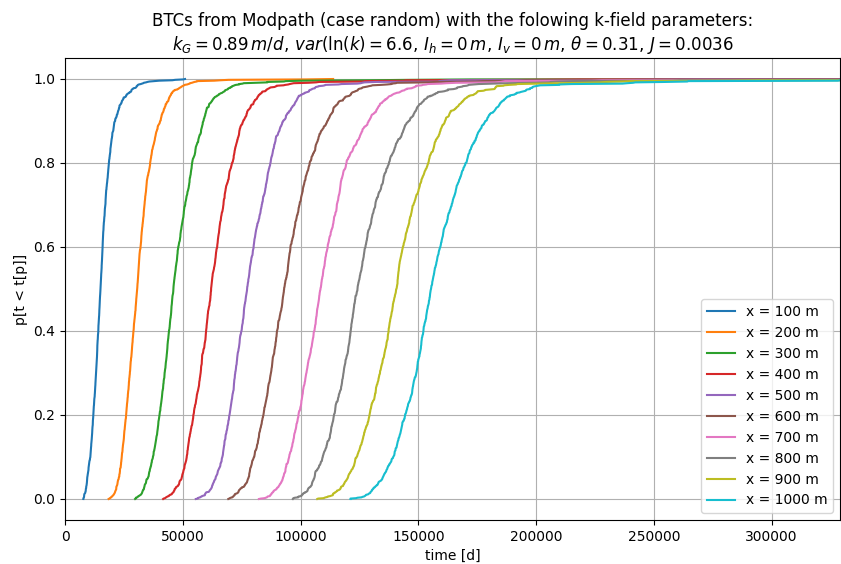


Figure 24: Breakthrough curves for different observation distances.

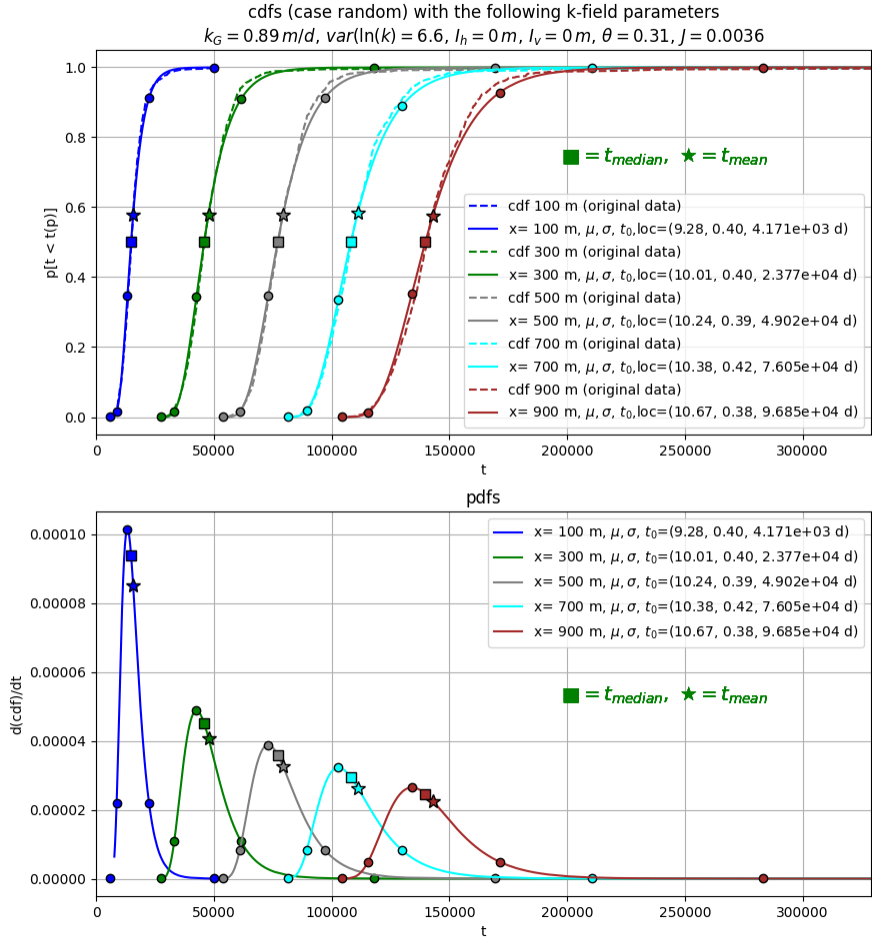


Figure 25: Top: Breakthrough curves with fitted cdfs. Bottom: Companian pdfs. The circles are at $t = t(t_{mode} - t_0)$ with $f = 0.2, 0.5, 1.0, 2.0, 5.0$.

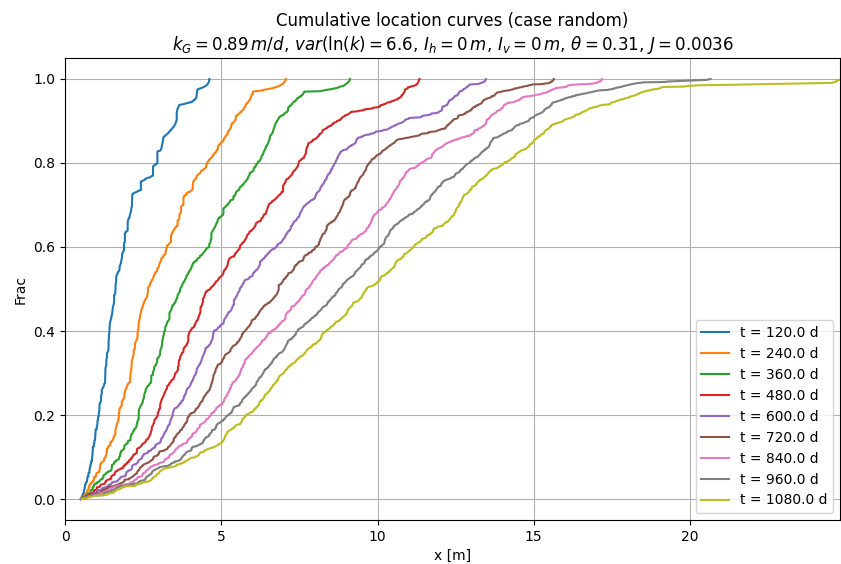


Figure 26: Cumulative location curves for different observation times.

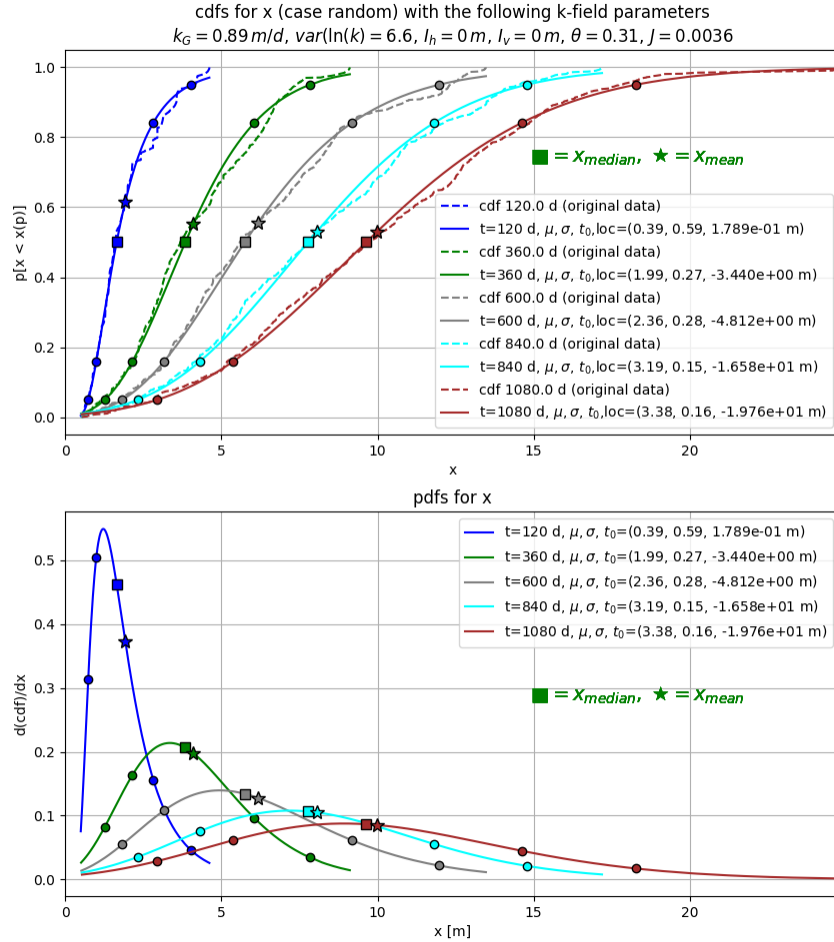


Figure 27: Top: Cumulative location curves for different observation times with fitted csfs. Bottom: Accompanying pdfs. The circles are at $cdf = p$ where $p = 0.05, 0.16, 0.5, 0.84, 0.95$.

5.6 Aquifer according to De Lange

To construct a cross section that complies with the concept developed by De Lange (2020, 2022), we have to choose domains A (mixing boxes) with L about $6 \lambda_h$ and D about $6 \lambda_v$, given the hint by De Lange that the scale factor N is about 3, while according to his papers $L_A = 2\lambda_h N$ and $D_A = 2\lambda_v N$ with λ_h and λ_N the horizontal and vertical correlations lengths of the realworld aquifer. But what is not clear, is how to include both the low conductivity zone and the high conductivity zone in a single domain or, for that matter, in a single cross section? One could just generate the cross section with two zones in each domain, one low-k and one high-k zone and position them at random within each domain. Or, one could generate mixing boxes with either a high-k or a low-k zone in them and randomly position these boxes in the cross section. Or one could split the aquifer in two parts, an upper half and a lower half, and fill the upper half with high-k domains and the lower half with low-k domains, and afterwards collect all the particles. But at the same time, we would like to maintain the transmissivity of the entire aquifer the same. It is not clear how to do this, except for running the model and use the computed flow to scale back the result. But then we'll loose the link with the lognormal distribution of the real-world aquifer. Therefore, in fact, I have no clue of how to

do this. The most logical approach in my opinion, is to simply use a conductivity field that is geostatistically generated with the given real-world aquifer correlation lengths and its lognormal conductivity distribution, which is in fact, what I did already in one of the examples above.

I conclude, the simulation with the random conductivity field, with the correct correlation lengths and conductivity, probability is the conductivity field that should generate the most realistic breakthrough curves, which then should be in accordance with De Lange's conceptual model.

Nevertheless, in his papers, simulates the dispersion using an artificial aquifer consisting of mixing blocks, he calls domains, of given size that are placed next to each other and on top of each other thus filling up the entire cross section of the aquifer. Each block has a low background conductivity and includes an elongated facies with a high conductivity. The background and high facies conductivities are the same in each block. For this example they are chosen to be 5 and 500 m/d respectively.

Like in the previous examples the cross section has the same size, 100 m deep and 1000 m wide with cells of 1x1 m². Each block was given the size of 20 cells along the x-axis and 5 cells along the z-axis. The facies was placed randomly inside each block. The inner facies was given the size of 20 cells along the x-axis and 1 cell along the z-axis. This is about what De Lange uses in his example pictures. The boundary conditions are the same as in the previous examples, a gradient of 0.0036 and a porosity of 0.31. The results of the simulation are in the following pictures. Figure 28 shows the $\ln(k)$ field, i.e. one background conductivity and one facies conductivity according to the header of the figure. Figure 29 shows the streamline and the head contours. The high-conductive inclusions clearly distort and channel the flow through them. Figure 30 shows the cumulative breakthrough curves for different locations along the cross section. They are not symmetric due to the heterogeneous character of the aquifer. However, the asymmetry of the time-breakthrough curves at different observation locations can be deemed not so high as expected. The same conclusion can be drawn from the histograms in figure 31 they are far less asymmetric than expected. Therefore, they might be reasonably modelled by a more traditional Fickian model. Perhaps the number of inclusions or their lengths are too small to deem this aquifer a really heterogeneous despite the large contrast between the background and the facies conductivities.

The breakthrough curves for the different observation distances in the top of figure 20 show that the lognormal distribution fits very well through the modeled breakthrough curves. The corresponding pdfs at the bottom of figure 20 also show only moderate skewness. Perhaps strangely enough, the breakthrough curves (or cumulative location curves) for different observation times in the top of figure 21 don't fit well to the lognormal distribution. Their shape reveals the effect of preferential flow paths in these graphs that show the location of the particles at different moments. The corresponding pdfs are strongly skewed, contrary to those in figure 20. The skewness of the pdfs unveils the preferential flow paths with a limited part of the flow traveling at a high rate and the bulk lagging behind at a low rate caused by the 100 times lower background conductivities applied in this example. Yet figure 21 also shows that the distances traveled at the different observation times are small compared to the length of the cross section of 1000 m. This contrasts largely from the distance travelled by the particles captured at the different observation locations which varied from 100, 200, ... 1000 m and was the same for all particles at each given distance. This may imply that for the small distances the mixing as a process is too limited, given the length of the inclusions of 20 m. The very strong skewed character of the pdfs for the different observation times, which represent the most likely distribution of the pollution plume released at $t = 0$ and $x = 0$ bear a large comparison to the large skewness in observed plume spreading in heterogeneous locations as the Made site.

One thing to do is to set up the cross section in this example according to the theory of [De Lange (2020), De Lange (2022), De Lange (2025)] such that it reflects the properties at the Made site.

The geometric mean conductivity of the Made site is $k_G = 0.89$ m/d while $\sigma = 2.7$ on log scale, implying a factor $\exp(2.7) \approx 13$ on real-world scale. This implies a high conductivity $k_h \approx 11.6$ and a low conductivity $k_l \approx 0.068$ m/d. Now we will simply put those zones in the domains pairwise, such that the geometric conductivity remains about the same.

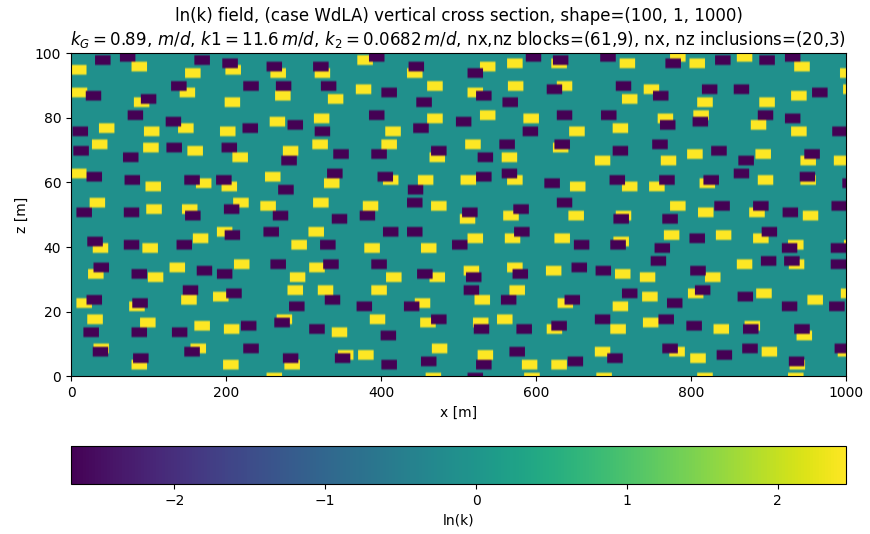


Figure 28: Conductivity field with background and facies data given in the header.

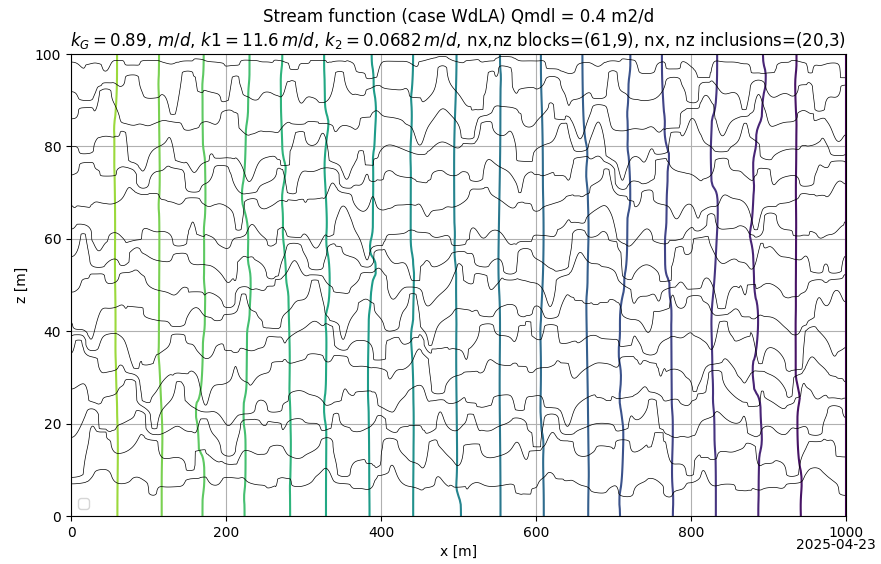


Figure 29: Streamlines and head contours for the simulated cross section. Only every 5th particle is shown.

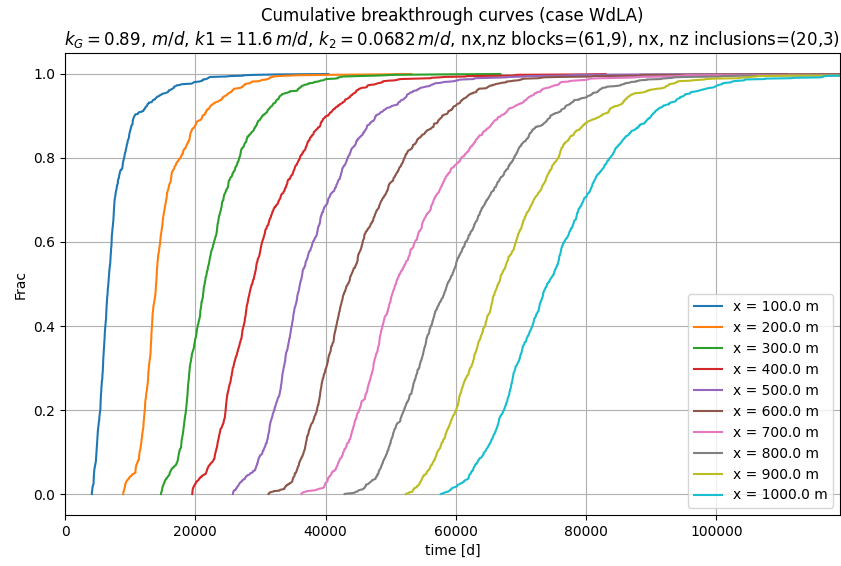


Figure 30: Cumulative breakthrough curves at different locations along the cross section

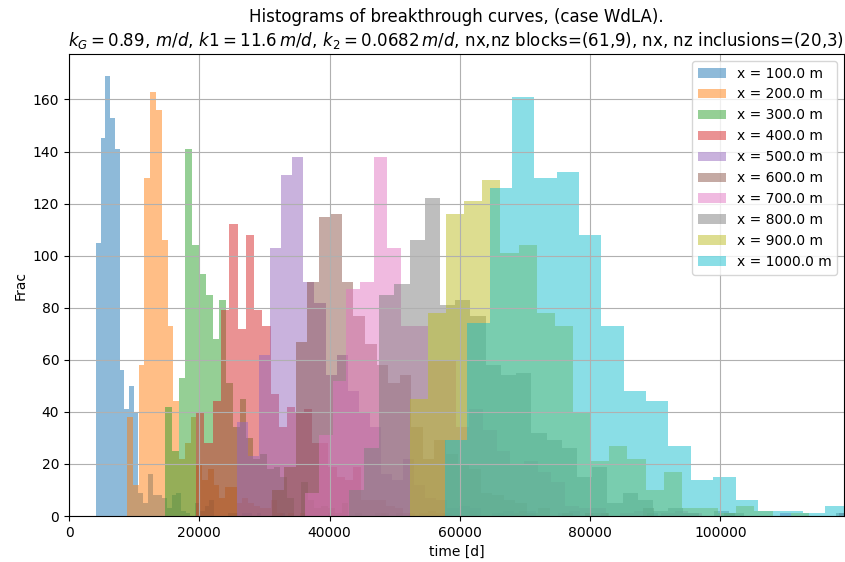


Figure 31: Histograms of different breakthrough points along the cross section

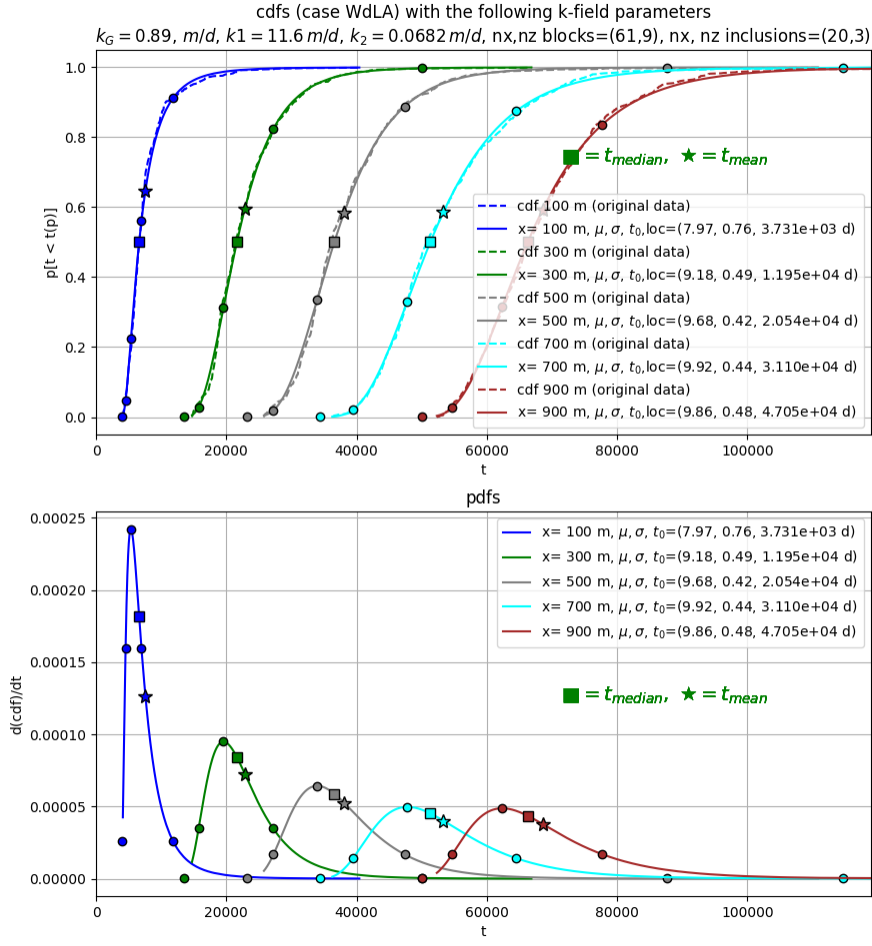


Figure 32: Top: Breakthrough curves from the model and fitted cdःs. Bottom: Pdfs corresponding to the fitted cdःs. Note that for the lognormal distribution $t_{mode} < t_{median} < t_{mean}$ as indicated. The circles are plotted at $t = t_0 + f(t_{mode} - t_0)$ with $f = 0.2, 0.5, 1.0, 2.0, 5.0$, where t_0 is the lowest possible value for the lognormal distribution ($t_0 = loc$) where loc is one of the parameters given by the fitting of the computed data.

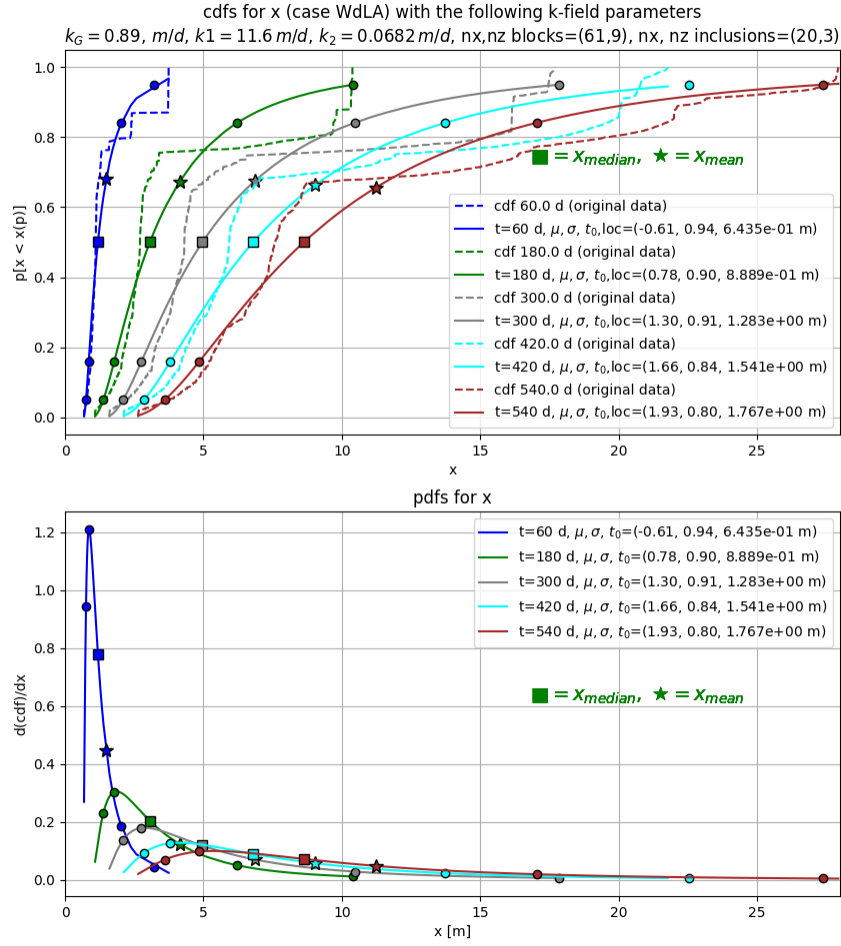


Figure 33: Top: Cumulative distribution of particles for different times as a function of x . The fit is not very good for this type of cross section, contrary to the break-through curves for different x as a function of time. The fitted pdfs clearly show a large skew relative to those for the breakthrough at different values of x in the previous figure. Note that the traveled distance at the observation times is really short compared to the length of the cross section, while the particles that were captured at the different observation locations have all traveled a much larger distance through the model.

5.7 Test case

It's important to run a test case that allows verification of the procedures developed for this work. The chosen test case has the same cross section of 100 rows and 1000 columns with cells of $1 \times 1 \text{ m}^2$. The aquifer is, therefore, 100 m thick and 1000 m long. The porosity is kept the same as before. The fixed gradient of $J = 0.0036$ was maintained. The section was divided into 10 blocks each consisting of 10 model layers. The conductivity is constant in each block and increases in 10 steps from 1 m/d to 10 m/d . Hence, the first 10 model layers all have $k = 1 \text{ m/d}$, the model layers 11 through 20 all have $k = 2 \text{ m/d}$ and so on until layers 91 through 100, which all have $k = 100 \text{ m/d}$. With this setup, the discharge through each layer and the travel time in them as well as the location of each particle at any time are now known and the model outcomes can now be verified by simple hand calculations.

The mean conductivity of this setup equals $k_{mean} = 5.5 \text{ m/d}$ and the total discharge $Q = k_{mean} \times D \times J = 0.55 \times 100 \times 0.0036 = 1.98 \text{ m}^2/\text{d}$. The Modflow listfile gives $1.98 \text{ m}^2/\text{d}$. The hand-computed travel times are also essentially the same as the ones computed by Modflow for all observation distances and for all layers. Finally the hand-calculated positions of the particles at the chosen observation times are essentially equal to the postions calculated by Modpath.

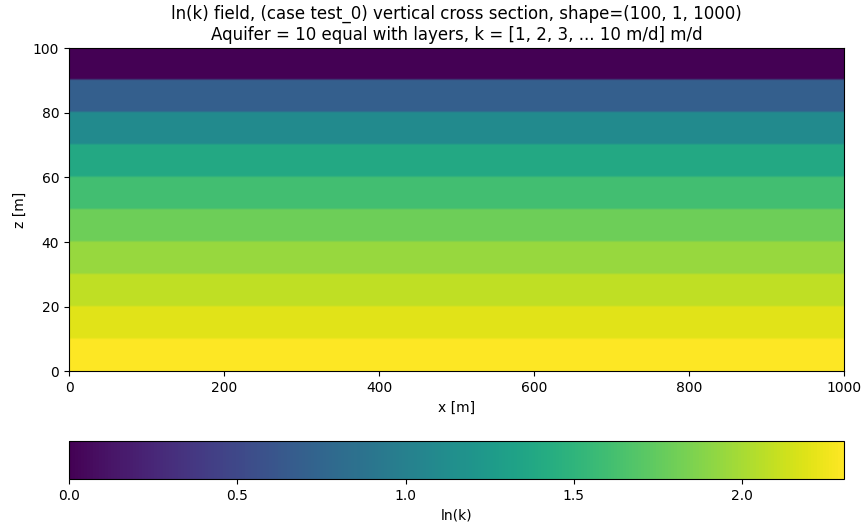


Figure 34: Conductivity field of the test case.

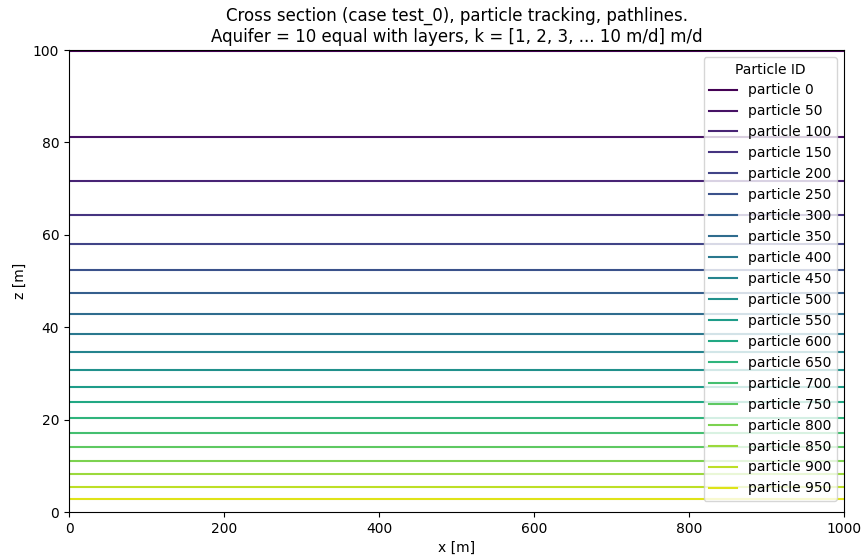


Figure 35: Path lines test0. The difference in distance between the path lines is because each path line represents the same fraction of the total discharge through the cross section.

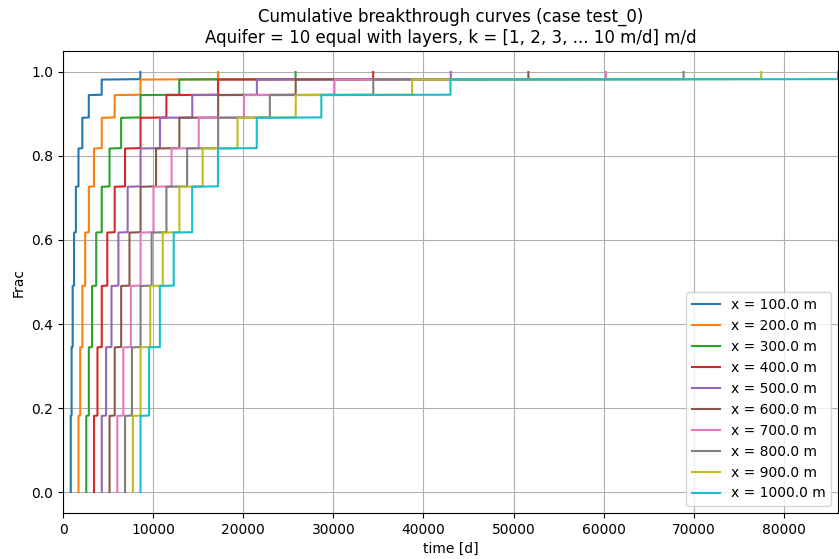


Figure 36: Break-through curves

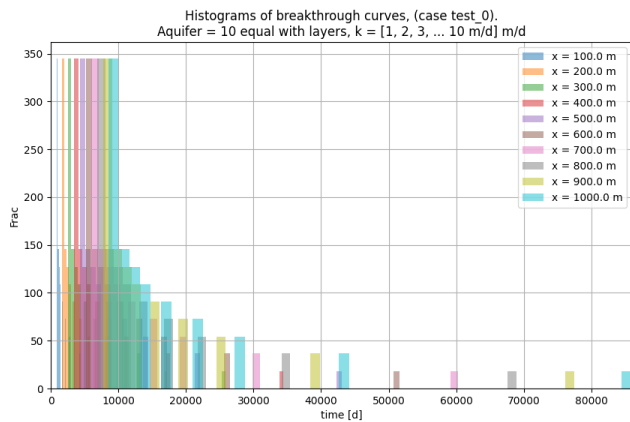


Figure 37: Histograms for breakthrough times

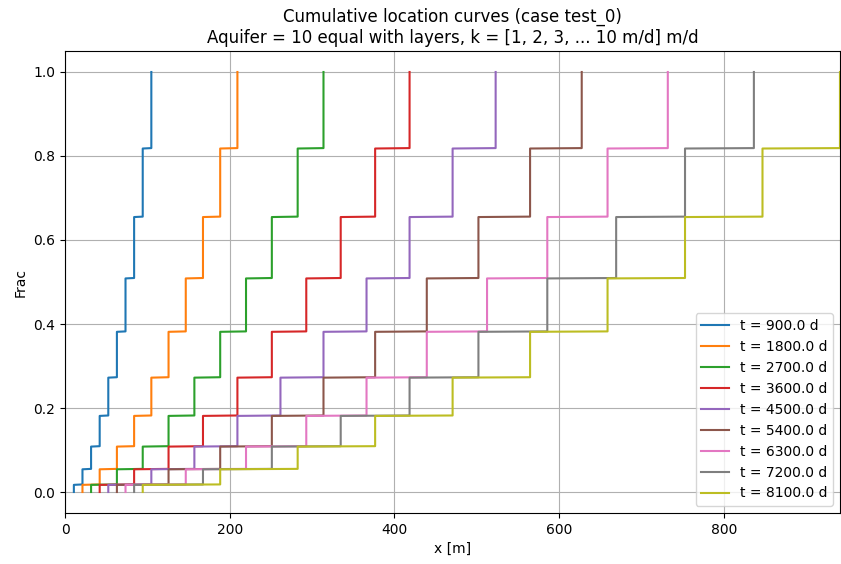


Figure 38: Cumulative location curves.

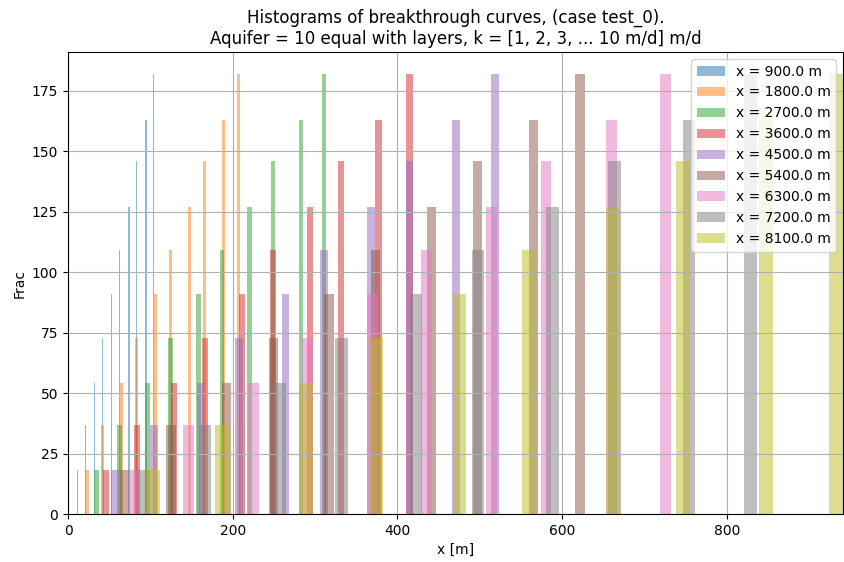


Figure 39:

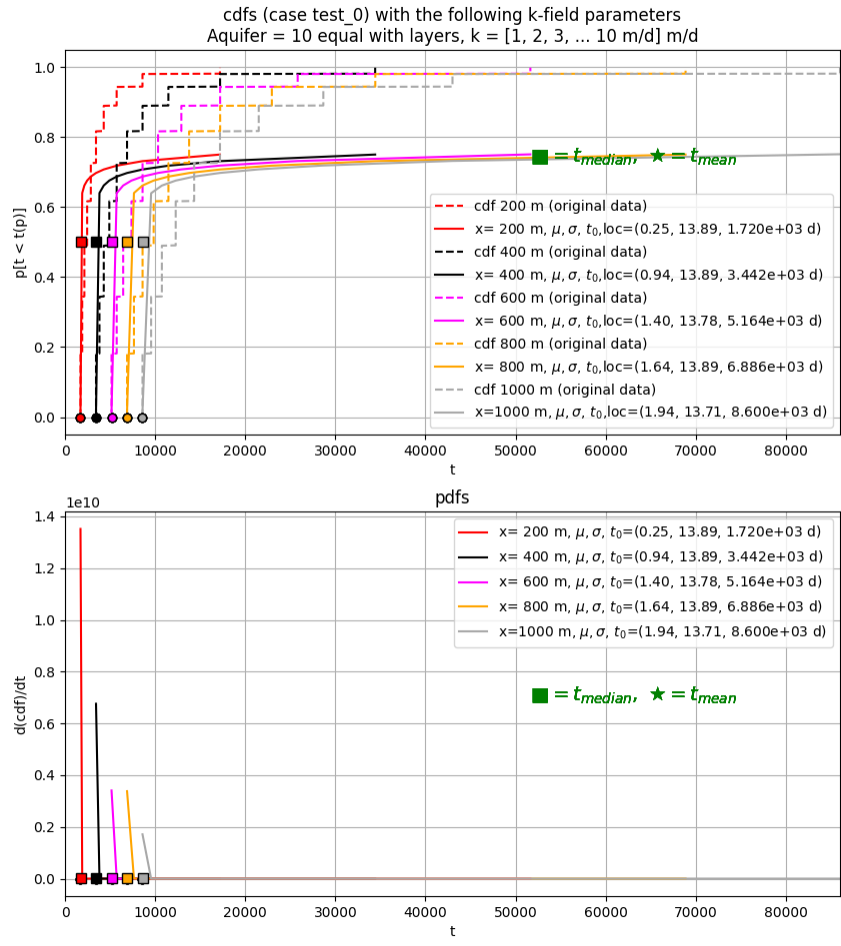


Figure 40: Fitted cdfs and their pdfs. Fit fails with this data (data that is essentially not random)

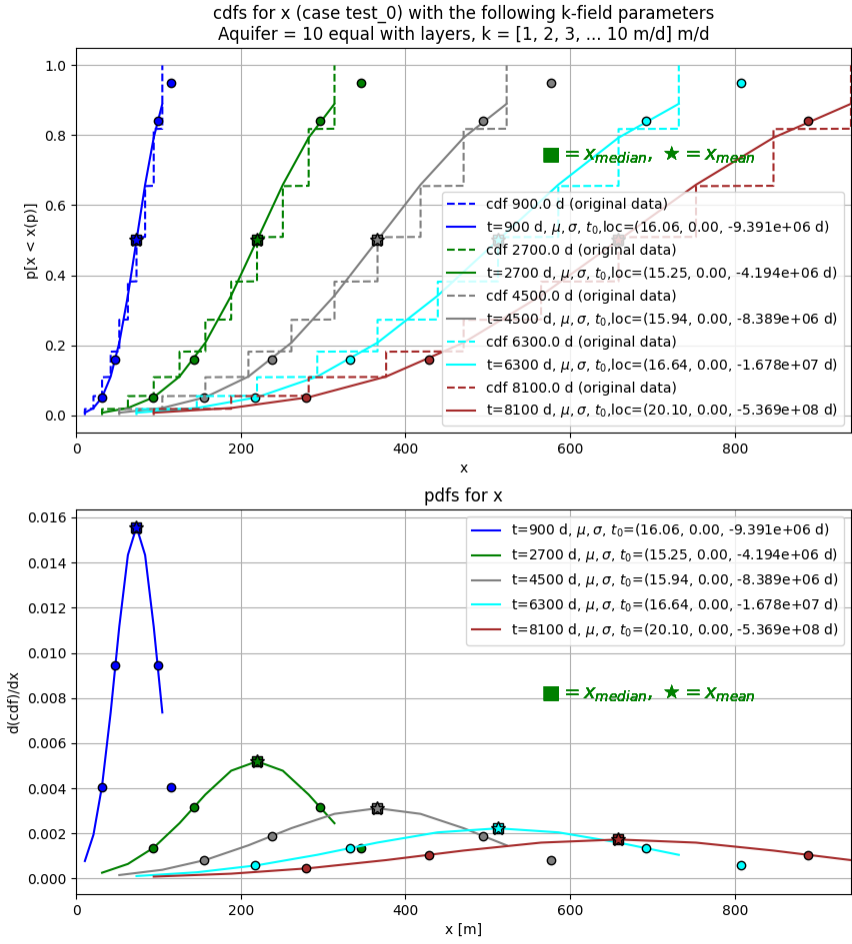


Figure 41: Fitted location curves. Works but is useless with this non-random test case.

6 Summarizing the discussion on dispersion

A phenomenon, including that of dispersion of a pollutant in moving groundwater, can often be best understood by looking at its behavior in extreme situations. We may, therefore, ask ourselves how dispersion develops in the following two extreme cases:

- Uniform flow in a perfectly homogeneous aquifer, with grains as fine as the water molecules themselves. Hence, there are no velocity variations.
- Flow in an aquifer that is layered and heterogeneous to the extreme. Hence, it consists of two parallel layers one with (almost) zero conductivity and the other with some distinct conductivity.

Over these cases, we may drape the process of diffusion, which is known to always work and does so at its own pace, irrespective of the actual velocity of the groundwater itself.

In the first case, the only movement of particles is the progress of the front, initially flat and perpendicular to the flow, which will always remain sharp and stay perfectly flat. The only thing diffusion does is to cause some spread in longitudinal direction. Without diffusion, the breakthrough curve would be vertical. With

diffusion it would still be very steep. The breakthrough curve would be fully described by the average front position and its standard deviation $\sigma = \sqrt{2D_d t}$. Even if the particles would be subject to some small-scale random velocity variations, the front will have the same properties, with a σ that will be larger than that caused by molecular diffusion, probably even be much larger, but would still follow this expression $\sigma = \sqrt{2Dt}$. Only now we have $D = D_v + D_d$ and since the random velocity differences are proportional to the groundwater velocity itself, we would have $D = a_L v + D_d$ and the process would be fully Gaussian and Fickian, with a head and tail of the same length and shape.

In the second extreme case, a part, maybe half of the water will be funneled through the high-conductive layer, with the rest lagging far behind in the low-conductivity layer. When we call the situation at some point in time also a plume, we see that we have a head and a tail that are completely defined by the velocities in these two layers. Let the velocity in the two layers be v_1 and v_2 with conductivities k_1 and k_2 respectively and a gradient i and porosity θ , we have

$$\begin{aligned} v_1 &= k_1 i / \theta \\ v_2 &= k_2 i \theta \end{aligned}$$

The total discharge through the aquifer then equals

$$Q\theta = D_1 k_1 i + D_2 k_2 i = D k_m i$$

With D_1 and D_2 the thicknesses of the respective zones and D the aquifer thickness.

Assume that the same amount of water flows through both zones, so that $D_1 k_1 = D_2 k_2$

$$\begin{aligned} k_m &= 2 \frac{D_1}{D} k_1 \\ k_m &= 2 \frac{D_2}{D} k_2 \end{aligned}$$

We are still free to choose k_1/k_2 or D_1/D_2 or D_1/D for that matter. Just take $D_1 = 0.1D_2$ so that $k_1 = 10k_2$ then

$$\begin{aligned} k_m &= 2 \frac{0.1}{1.1} k_1 \approx 0.19 k_1 \rightarrow k_1 \approx 5.3 k_m \\ k_m &= 2 \frac{0.9}{1.1} k_2 \approx 1.64 k_2 \rightarrow k_2 \approx 0.61 k_m \end{aligned}$$

We could even take a more extreme case in which $D_1 = 0.001D_2$ so that $k_1 = 1000k_2$ yielding

$$k_m = 2 \frac{0.001}{1.001} k_1 = 2 \frac{0.999}{1.001} k_2 \approx 0.002 k_1 \approx 2 k_2$$

in which still half of the discharge flows through the thin conductive layer and the other half through the thick layer with the low conductivity. In these cases, even when equal amounts of water pass through both zones, the distance traveled in the fast, high-conductive zone is more than 5 to 500 times the average traveled distance, and the distance traveled in the low-conductive zone is about 60% to 50% of the average traveled distance, where 50% is the limiting case.

What happens if we sample the water by means of a well that extracts all the water at a certain point? Then, as soon as the fast front passed this point, the relative concentration would jump to 0.5, to remain constant until the tail passes, at which point the relative concentration would jump further to 1.0. From these samples one could conclude that the mean of the front would lie half way between the two mentioned times and that its spread would amount to $\sigma = \frac{t_1 - t_2}{\sqrt{2}}$. On the other hand, if one samples the aquifer without actually extracting water by a well (volume sampling as it is called by [Maas (1994)], for instance by means of a device that measures some quality aspect in situ at any depth, and if we then take the mean along the vertical, a completely different breakthrough curve would emerge. As the fast zone has only one tenth or even one thousandth of the thickness of that of the slow zone, the relative concentration would, after passing

the sampling location, only jump up to 0.1 or to 0.001 instead of 0.5 and would rise to 1. 0 after passage of the front in the slow zone. Therefore, the way of sampling may make a huge difference in the outcomes.

What also jumps into mind in this extreme case, is, that the spread, i.e. the distance between head and tail, grows proportionally to time and, therefore, with distance. In the case of Fickian dispersion it grows proportional to the root of time, which is equivalent to the root of the travelled distance given that $\sigma = \sqrt{2Dt} \approx \sqrt{2avt} = \sqrt{2aL}$. Reality will likely pop up somewhere in between.

If we drape diffusion or our ignored random small-scale velocity variations over the last situation, there will be some longitudinal dispersion, which may be negligible relative to the fast moving head of the front. However, we will also see some dispersion across the horizontal line that separates the two zones. The importance of this sideways spreading depends on the magnitude of the process, or perhaps on the absolute speed of the groundwater relative to diffusion. Nevertheless, if one imagines a very large sideways diffusion, it would cause the head of the front to loose concentration to the water in the slow zone. The larger this process, the more the end result will resemble Fickian behavior.

Now imagine that the fast zone were split into a vast number of subzones spread out over the vertical, but still making sure that the combined transmissivity of these fast subzones remains equal to that of the original one. This would make diffusion dominant instead of negligible, even with the same overall transmissivities, conductivities and zone thicknesses; it would, therefore, completely alter the shape of the front. Hence, size or layering matters. This also includes time because time affects the size of the spread by diffusion, which, as we have seen, will grow to aquifer-height proportions if sufficiently long. Even much shorter times may be important if the fast and the slow layers are thin. Reality will always be somewhere in between. The more homogeneous the aquifer, or the thinner the layers, the more Fickian the dispersion process will be. The more heterogeneous in the sense that the flow is more dominated by preferential flow paths, the less Fickian the dispersion will be, and the more its spread will grow linearly with time and distance. Because the streamlines in real-world cases will pass through sequences of zones of higher and lower conductivities of different extent, the spread may grow towards linear with traveled distance, the larger the probability of encountering high-conductivity zones of even larger extent that channel the groundwater along preferential paths.

But in any case, as long as the dispersion is a random process, the breakthrough curves will tend to the normal distribution the longer the travel distance as demanded by the central limit theorem. The examples given also show this behavior.

7 Summary and conclusions

Dispersion during subsurface mass transport was studied based on recent papers as mentioned in the references. The phenomenon of dispersion is still not totally tackled in models as well as in theory. [Zheng et al. (2011)] mentioned the dual medium feature, adding kinematic sorption, that was built into the MT3DMS mass transport model to better capture the observations of tracer tests in the Made test site [Zheng et al. (2011)]. However, the improved match may well have been reached for the wrong reasons, as there was no sorption active at the site during the bromium tracer test. At least [Fiori et al. (2013)] showed that a similarly accurate result could be reached with their MIM (multi indicator model), which only took advection into account. The problem is believed to have been the impossibility to characterize and model the heterogeneous conductivity field in the subsurface accurately enough, because therein seems to lie the key to successfully model subsurface displacement of pollutants and successfully include match the observed dispersion.

It is generally known that in real-world situations flow along preferential paths is often dominant. At the same time, it is extremely hard to predict beforehand based on methods available to characterize the subsurface's conductivity field in all three dimensions. While in more homogeneous aquifers dispersion tends toward Fickian behavior, in heterogeneous aquifers it does not. Fickian behavior sees dispersion as a Gaussian process, which yields symmetrical breakthrough curves and histograms with the spread that grows according to the square root of the traveled distance. However, non Fickian behavior as observed in heterogeneous aquifers, show asymmetrical breakthrough curves and histograms, with early breakthrough and a large tail, with an associated spread that grows linearly with travel distance.

This non-Fickian behavior was shown by modelling a heterogeneous aquifer with the properties of the

Made site ([[Fiori et al. \(2013\)](#)]). The aquifer generated with those parameter values, was similar to that by which [[Fiori et al. \(2013\)](#)] were able to reasonably well model the bromide tracer test at the Made site. The results show indeed that the breakthrough curves and breakthrough histograms have an early breakthrough with a long tail. The opposite, more Fickian result was obtained by modeling another cross section generated with the same parameters, but with a far lower $\ln(k)$ variance, which resulted in a much more homogeneous aquifer. The aquifer used by [[Fiori et al. \(2013\)](#)] consisted of blocks with a length of around 20 m based on the horizontal integration scale (range of the semi-variogram). Each block got a conductivity value chosen from a generated random field with the proper statistical values. In the third example, we left the block structure out and directly used the statistically generated conductivity field with the same properties and integration lengths. The results show that the results are similar to those of the first example that was generated with the same statistical parameter values (see the header of each figure for the values used). Hence, using the block structure does not seem to add much to the results; only the horizontal and vertical semi-variograms used to generate the random field seem to matter.

As a fourth example, a purely random field was generated with the horizontal and vertical integration length both zero. The conductivity of each model cell as independently selected from the lognormal distribution with the same mean and variance as the previous three examples. This example shows the most symmetrical breakthrough curves the pdfs of which are most similar to the normal distribution.

It was observed that the location curves, i.e. the particle position at given observation times are much more symmetrical than the time-breakthrough curves obtained from the same simulation. Moreover, those curves are virtually symmetric for both the case with zero as with nonzero integration lengths. This is an observation without underlying theory to explain this behavior.

Finally, a cross section was generated alike the one De Lange uses in his papers to demonstrate and simulate dispersion in very heterogeneous aquifers. De Lange, for the sake of modelling dispersion, sees the aquifer as layers of equally sized blocks called domains, which are put next to and on top of each other to fill the aquifer. Each block has a low background conductivity (of 5 m/d) and holds an elongated, rectangular inclusion with a high conductivity (of 500 m/d). This cross section was simulated in the same way as the previous ones. Expected was a strong non-Fickian behavior to show up in the breakthrough curves and the histograms. However, this proved hardly the case. So perhaps the cross section was not heterogeneous enough, despite the 100-fold conductiviy contrast between the background and the included facies conductivities.

8 Analysis of the lognormal distribution

$$\text{if } T \sim \text{LogNormal}(\mu, \sigma) \rightarrow \log T \sim N(\mu, \sigma)$$

When retrieving the lognormal distribution or generating it, it has three parameters scale, loc, shape, where

$$\mu = \ln(\text{scale})$$

$$\sigma = \text{shape}$$

loc=linear shift in the time domain (real world domain)

$$t \sim \text{LogNormal}(\mu, \sigma, \text{loc})$$

is equivalent to saying

$$\ln(t - \text{loc}) \sim N(\mu, \sigma^2)$$

Or, rearranged

$$t = \text{loc} + \exp(X), \quad X \sim N(\mu, \sigma^2)$$

1. Hence, *loc* acts as a shift in the time domain.
2. It's the minimum value the variable *t* can take – the distribution is defined for $t > \text{loc}$.

3. It's often used to delay the onset of the lognormal process.

Further properties of the lognormal distribution

$$\text{mean}(t) = \text{loc} + \exp\left(\mu + \frac{\sigma^2}{2}\right)$$

$$\text{median}(t) = \text{loc} + \exp(\mu)$$

$$\text{mode}(t) = \text{loc} + \exp(\mu - \sigma^2)$$

Head and tail quantiles may be useful, but more so in log-space than in real-space due to the skewness of the lognormal distribution. The quantile times $s t_{05}, t_{16}, t_{50}, t_{84}$ and t_{95} can also easily obtained from a given cdf or pdf distribution, but these too are less informative for the lognormal distribution than for the normal distribution.

Table 1: Head and tail quantiles

Region	Log-space range	Time space rang
Head	$\mu - 2\sigma$ to $\mu - \sigma$	$[e^{\mu-2\sigma}, e^{\mu-\sigma}]$
Bulk	$\mu - \sigma$ to $\mu + \sigma$	$[e^{\mu-\sigma}, e^{\mu+\sigma}]$
Tail	$\mu + \sigma$ to $\mu + 2\sigma$	$[e^{\mu+\sigma}, e^{\mu+2\sigma}]$

Let x be the traveled distance, then

Table 2: Velocities

Time statistic	Velocity=distance/time	Behavior
Mean	$v_{\text{mean}} = x / (\text{loc} + \exp(\mu + \sigma^2/2))$	Roughly constant → average advection
Mode	$v_{\text{mode}} = x / (\text{loc} + \exp(\mu - \sigma^2))$	Decreases with increasing x , since the distribution skews more. Early arrivals shift right as distance increases (due to dispersion)

Physical interpretation:

- The mean reflects the center of mass of the particle plume.
- The mode reflects the most probable arrival time, which is more sensitive to early or delayed arrivals due to dispersion.
- When the mean velocity remains constant confirms a linear advection front.
- The mode shifts sublinearly with distance implies that the spread (dispersion) becomes more significant with distance, skewing the distribution more and pushing the peak back.
- The median is the time at which the cdf=0.5 as half the particles take shorter and the other half longer than this time.
- The mean velocity is equal to the surface to the left of the cdf. This too is obvious.
- The model is the time at which the cdf is steepest, i.e. its first derivative peaks (this is obviously the top of the pdf).

An easy and informative criterion for early and late arrivals may be built on loc as the earliest possible moment of arrival of particles and t_{mode} as the most probable time of arrival. We may select point based on the ratio of these two times. Let's, just for convenience rename loc

$$t_0 = \text{loc}$$

then we can base arrival time criteria on the ratio

$$\alpha = \frac{t - t_0}{t_{mode} - t_0}$$

and so

$$t = t_0 + (t_{mode} - t_0) \alpha$$

and use the following arrival criteria

Table 3: Arrival criteria

α -range	Arrival type
0.0 – 0.2	Very early arrivals
0.2 – 0.5	Early arrivals
0.5 – 2.0	Normal arrivals
2.0 – 5.0	Late arrivals
> 5.0	Very late arrivals

References

- [Bowling et al. (2005)] Bowling, J.C., Rodriguez, A.B., Harray, D.L., Zheng, C. (2005) Deliniating Aluvial Aquifer Heterogeneity Using Resistivity and GPR Data. *Ground Water*, Vol. 43, No. 6. p890-903.
- [Coe (2003)] Coe, A.L. (2003) The sedimentological record of sea-level change. Cambridge University Press, Cambridge UK. ISBN 0-521-53852-4. 279p.
- [Fiori et al. (2013)] Fiori, A., Dagan, G., Janković, I. & Zarlenga, A (2013) The plume spreading in he Made transport experiment: Could it be predicted by stochastic models? *WRR*, Vol. 49, 1-11, doi:10.1002/wrcr.20128 2013.
- [Hemker and Bakker (2004)] Hemker, C. J., Van den Berg, E., & Bakker, M. (2004). Ground water whirls. *Ground Water*, 42(2), 234–242.
- [Jankovic et al. (2010)] Janković, I., & Fiori, A. (2010). Anomalous transport in highly heterogeneous 3D aquifers: A numerical study. *Water Resources Research*, 46(10), W10502. <https://doi.org/10.1029/2009WR008839>
- [Jankovic et al. (2006)] Janković, I., Fiori, A., & D. Dagan (2006) Modeling flow and transport in highly heterogeneous three-dimensional aquifers: Ergodicity, Gaussianity, and anomalous behavior. I Conceptual issues and numerical simulations. *WRR*, Vol.42, W06D12, doi:10.1029/2005/WR004734. 9p.
- [Jankovic et al. (2003)] Janković, I., Fiori, A., & Dagan, G. (2003). Flow and transport in highly heterogeneous formations: 3D numerical simulations and the validity of the Boussinesq approximation. *Water Resources Research*, 39(3), 1045. <https://doi.org/10.1029/2001WR001182>

- [Jensen et al. (1993)] Jensen K. Hogh & Bitsch K. (1993) Large-scale Dispersion Experiments in a Sandy Aquifer in Denmark: Observed Tracer Movements and Numerical Analysis. WRR Vol.29, No. 3, 673-696
- [De Lange (2025)] Lange, W.J. de (2025) Using Advective Transport Phenomena In Modeling To Better Understand Mechanical Dispersion: Step One. In preparation.
- [De Lange (2022)] Lange, W.J. de (2022) Advective Transport Phenomena to Better Understand Dispersion in Field and Modeling Practice. Groundwater 58, 46–55. <https://doi.org/10.1111/gwat.12883>
- [De Lange (2020)] Lange, W.J. de (2020) Advective Transport Phenomena to Better Understand Dispersion in Field and Modeling Practice. Groundwater 58, 46–55. <https://doi.org/10.1111/gwat.12883>
- [Maas (1994)] Maas, C (1994) On Convolution Processes and Dispersive Groundwater Flow. PhD Thesis TU-Delft, 13-June 1994.
- [Sudicky (1986)] Sudicky EA (1986) A Natural Gradient Experiment on Solute Transport in a Sand Aquifer: Spatial Variability of Hydraulic Conductivity and Its Role in the Dispersion Process. WRR 22(1986)13, 2069-2082.
- [Zheng et al. (2011)] Zheng, C., Bianchi, M. & Corelick S.M. (2011) Lessons Learned from 25 Years of Research. Review paper. Ground Water, 29(5), 649-662. [#8203](https://doi.org/10.1111/j.1745-6584.2010.00753.x)